

# Quantum Simulator with Circular Rydberg Atoms

Report about my summer internship at the University of Warsaw  
written by

**Paula Heim**

**August and September 2023**

# Contents

<b>1</b>	<b>Introduction</b>	<b>2</b>
<b>2</b>	<b>Circular Rydberg and Magnetic Atoms</b>	<b>3</b>
2.1	The proposed system . . . . .	3
2.2	The effective Hamiltonian . . . . .	5
2.3	The problem with the proposed system . . . . .	6
<b>3</b>	<b>Multiple Circular Rydberg Atoms</b>	<b>7</b>
3.1	The proposed system . . . . .	7
3.2	The effective Hamiltonian . . . . .	10
3.3	Simulating the dynamics . . . . .	11
3.4	Alternative states selection . . . . .	17
3.4.1	The system . . . . .	17
3.4.2	The interaction coefficients . . . . .	20
<b>4</b>	<b>Data</b>	<b>25</b>
4.1	Different small considerations . . . . .	25
4.2	Dependence of $J$ 's on various control parameters for the system using only circular states . . . . .	27
4.2.1	$J_{zz}$ . . . . .	28
4.2.2	$J_{+-}$ and $J_{-+}$ . . . . .	30
4.2.3	$J_{+-}/J_{zz}$ . . . . .	32
4.2.4	$J_{z+}$ and $J_{z-}$ . . . . .	34
4.2.5	$J_{+z}$ and $J_{-z}$ . . . . .	36
4.2.6	$J_{++}$ and $J_{--}$ . . . . .	38
4.3	Histograms of eigenvalue differences . . . . .	40
	<b>References</b>	<b>42</b>

# 1 Introduction

Ultracold atoms provide a platform for quantum computing. Among the promises of the field is the possibility to experimentally simulate many body systems, which are, due to the size of their Hilbert space, often computationally not traceable. Ultracold atoms allow us to control the accessible quantum states and their interactions precisely, therefore enabling us to simulate a large number of different systems. Recently, more and more advances have been made in the field [Ngu+18].

Circular Rydberg atoms are particularly intriguing. Rydberg atoms are atoms with one highly excited electron, so that the quantum mechanical description resembles the hydrogen atom with some small corrections. Circular Rydberg atoms are Rydberg atoms where the excited electron is in a state with maximal angular momentum and magnetic quantum number. These atoms have large electric and magnetic dipole moments, enabling strong inter-particle interactions, and relatively large lifetimes, allowing to observe the resulting dynamics of the simulated many body system [Gal94].

The purpose of this project was to theoretically investigate a particular system of ultracold atoms which can serve as an experimental platform to simulate many body systems, where the constituents are two-state quantum systems, for example  $\frac{1}{2}$ -spin particles. Moreover, the proposed system consists of two types of particles, allowing to simulate many body systems with two types of two-body interactions. Generalisations to higher-spin particles are straightforward with this approach, although as the number of quantum states grows, more and more pitfalls could complicate an experimental realisation. In a first approach, I considered a system of one circular Rydberg atom placed in a bath of magnetic atoms, which should interact through magnetic dipolar interactions. However, it turned out that these interactions were too weak compared to the lifetimes of the circular Rydberg state, so that the dynamics would not be observable. In the second approach, I therefore considered an array of two species of circular Rydberg atoms with significantly different principal quantum numbers, and their electric dipolar interactions.

Together with Jacek Dobrzyniecki we expanded on this idea and exchanged one of the the circular-circular transitions with a transition between a circular and an elliptical Rydberg state<sup>1</sup>. This approach proved fruitful for the goal of finding an experimental system that can be used to simulate two-species many body systems, and in addition have easily tunable interaction parameters. Our preprint is available here.

I am grateful for the hospitality of the Faculty of Physics at the University of Warsaw, and in particular the members of Michał Tomza's Quantum Molecular Systems group, who made me feel very welcome during my stay and provided me with many stimulating discussions. I am also grateful for the supervision of my project by Michał Suchorowski.

My work was supported by a fellowship of the German Academic Exchange Service (DAAD).

---

<sup>1</sup>Elliptical Rydberg states are Rydberg states where the excited electron has magnetic quantum number one below the possible maximum.

## 2 Circular Rydberg and Magnetic Atoms

### 2.1 The proposed system

We consider a system that consists of one Rydberg atom in the circular state (meaning that the quantum numbers  $l$  and  $m$  are maximal, i.e. we have  $|n, l, m\rangle = |n, n-1, n-1\rangle$ ) and some magnetic atoms placed around it. A wide array of geometries can be realised with optical tweezers, thus we aim to make our considerations as generally applicable as possible. For explicit calculations, we choose our Rydberg atom to be a Rubidium atom (although for states with high angular momentum quantum numbers the potential is very well modelled by a hydrogen-like potential and the type of atom is therefore irrelevant). The magnetic atoms are taken to be Dysprosium atoms.

The excited electron generates a magnetic moment which interacts with the magnetic dipole moment of the magnetic atoms through magnetic dipole-dipole interaction,

$$\hat{V}_{dd} = \frac{\mu_0}{4\pi} \sum_{q, q'=-1}^1 v_{qq'}^{geom.}(\vec{r}) \hat{\mu}_q \hat{\mu}_{q'}$$

where the magnetic dipole operator  $\hat{\mu}_q$  acts on one particle,  $\hat{\mu}_{q'}$  on the other. We have for  $\vec{r} = (r, \vartheta, \varphi)$ , the difference vector of the positions of the two atoms,

$$v_{zz}(\vec{r}) = \frac{1 - 3 \cos^2 \vartheta}{r^3},$$

$$v_{+-}(\vec{r}) = v_{-+}(\vec{r}) = \frac{1}{2} \cdot \frac{1 - 3 \cos^2 \vartheta}{r^3},$$

and the other contributions vanish because for the proposed setup, the dipolar interaction conserves  $\mu_z$ . This can for example be made plausible by decomposing the operator in its most elementary (?) form

$$\hat{V}_{dd} = \frac{\mu_0}{4\pi} \cdot \frac{\hat{\mu} \cdot \hat{\mu} - 3(\vec{e}_r \cdot \hat{\mu})(\vec{e}_r \cdot \hat{\mu})}{\vec{r}^3},$$

where  $\vec{r}$  is the difference vector of the positions of the two atoms, into contributions including angular momentum of the relative motion of the two particles and those related to their magnetic moments. Due to the more or less fixed positions of the particles in the optical tweezers, the angular momentum of the relative motion cannot change and only the terms above remain.

We assume that the states of the Dysprosium atoms can be labelled by the z-component of their spin,  $|\Psi_{Dy}\rangle = |j, m\rangle$ , where we leave  $j$  fixed at some realistic value ( $j = 8$ , add the reference!), and  $-j \leq m \leq j$ . The magnetic moment operators  $\hat{\mu}_z, \hat{\mu}_+ = \hat{\mu}_x + i\hat{\mu}_y, \hat{\mu}_- = \hat{\mu}_x - i\hat{\mu}_y$  act on such

a state as follows,

$$\begin{aligned}\hat{\mu}_z |j, m\rangle &= \mu_B \hbar g_m m |j, m\rangle, \\ \hat{\mu}_+ |j, m\rangle &= \mu_B \hbar g_m \sqrt{j(j+1) - m(m+1)} |j, m+1\rangle, \\ \hat{\mu}_- |j, m\rangle &= \mu_B \hbar g_m \sqrt{j(j+1) - m(m-1)} |j, m-1\rangle.\end{aligned}$$

By  $\mu_B$  we denote the Bohr magneton and the prefactor  $g_m = 1.24159$  is taken from [KP11].

For the Rydberg atom, the corresponding relations are

$$\begin{aligned}\hat{\mu}_z |n, l, j, m_j\rangle &= \mu_B \hbar g_l m_j |n, l, j, m_j\rangle, \\ \hat{\mu}_+ |n, l, j, m_j\rangle &= \mu_B \hbar g_l \sqrt{l(l+1) - m_j(m_j+1)} |n, l, m_j+1\rangle, \\ \hat{\mu}_- |n, l, j, m_j\rangle &= \mu_B \hbar g_l \sqrt{l(l+1) - m_j(m_j-1)} |n, l, m_j-1\rangle.\end{aligned}$$

with the Landé-factor

$$g_j = g_l \frac{j(j+1) - s(s+1) + l(l+1)}{2j(j+1)} + g_e \frac{j(j+1) + s(s+1) - l(l+1)}{2j(j+1)},$$

and  $g_l = 1 - \frac{m_e}{m_{nucleus}}$ , and  $g_e \approx 2$  is the electron  $g$ -factor.

We apply a constant and homogeneous external electric and magnetic field  $\vec{E} = E\vec{e}_z, \vec{B} = B\vec{e}_z$ . The fields are always parallel and thus define the quantisation axis. The states of the magnetic atoms experience linear Zeeman shifts in the magnetic field whereas for the Rydberg atom, the electric field mixes states with different  $n, l$ , but  $m$  is still a good quantum number). The spectrum of the Rydberg atom can be seen in Figure 3. All states experience linear Zeeman shifts proportional to their magnetic quantum number  $m$ ,

$$\hat{H}_{Zeeman} = \hbar g_{Dy} \mu_B B \hat{S}_z.$$

The circular state shows a second order Stark shift due to the electric field and the three states with  $m = n - 2$  exhibit a linear Stark shift which splits their spectrum into three nondegenerate levels. The external fields are accounted for in the one-body Hamiltonians of the atoms.

The combination of these external fields can now be used to select two states, the circular state and one state with  $m = n - 2$ , from all the states of the Rydberg atom so that "spin exchange" (of the effective spin states, see below) between the Rydberg and the magnetic atoms is resonant, that is, the energy difference between two states in the magnetic atom equals the energy difference between the two selected states in the Rydberg atom. To choose such a combination, we plot the energy differences between the three levels with  $m = n - 2$  and the circular state together with the energy differences caused by the Zeeman shifts for  $E = 1V/cm$  as functions of  $B$  and look for the intersection. This can be seen in the following plot.

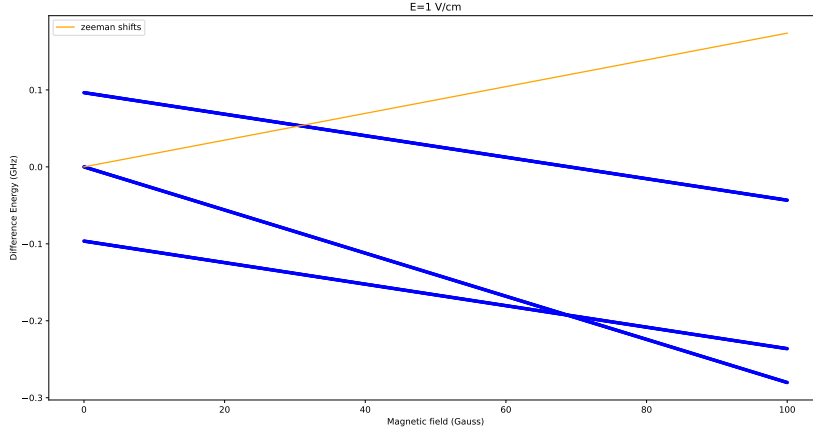


Figure 1: Blue: Energy differences to the circular state in the Rydberg atom, orange: energy differences of two neighbouring states of the magnetic atom

We select as  $|\uparrow\rangle$  the circular state and as  $|\downarrow\rangle$  the state whose energy difference to the circular state at certain values of the external electric and magnetic fields equals the energy difference between two states of the magnetic atom whose magnetic quantum number differs by one.

## 2.2 The effective Hamiltonian

Our goal is to rewrite the interaction in terms of a system of spin-1/2 variables with interactions between pairs of spins. To do so, we bring the interaction in the form

$$\hat{V}^{kk'} = \sum_{q,q' \in \{z,-,+\}} J_{qq'}^{kk'} \hat{S}_q^{(k)} \hat{S}_{q'}^{(k')}.$$

which, in the basis (3.5), is represented by the matrix

$$V_{spins}^{kk'} = \begin{pmatrix} \frac{1}{4}J_{zz} & 0 & 0 & 0 \\ 0 & -\frac{1}{4}J_{zz} & J_{-+} & 0 \\ 0 & J_{+-} & -\frac{1}{4}J_{zz} & 0 \\ 0 & 0 & 0 & \frac{1}{4}J_{zz} \end{pmatrix}. \quad (2.1)$$

The coefficients  $J_{zz}$  and  $J_{+-}$  take the form

$$J_{zz} = 2 \langle \uparrow\uparrow | \hat{V} | \uparrow\uparrow \rangle - 2 \langle \uparrow\downarrow | \hat{V} | \uparrow\downarrow \rangle$$

$$J_{+-} = J_{-+} = \langle \uparrow\downarrow | \hat{V} | \downarrow\uparrow \rangle.$$

Note that  $J_{zz}$  is independent of the quantum numbers  $n, l$  and  $m$  whereas  $J_{+-}$  scales as  $\sqrt{2n_k - 1}$ .

As in the discussion in Section 3.2, effective  $B$ -fields appear.

### 2.3 The problem with the proposed system

The problem with the proposed system: Assuming a distance of five times the peak in the radial part of the wave function of the circular Rydberg, we get the following matrix elements. The lifetimes curve corresponds to inverse lifetimes.

Some scaling relations for the circular states:

Quantity	Scaling with $n$
Lifetime	$n^5$
Radius where $R_{n,n-1}(r) = \max.$	$n^2$
$\langle m = n - 2   \hat{\mu}_-   m = n - 1 \rangle$	$\sqrt{2n - 1}$
$\langle m = n - 1   \hat{\mu}_z   m = n - 1 \rangle$	$n - 1$

Table 1: Power law dependencies of certain quantities of circular Rydberg atoms on the principal quantum number

These scaling relations show that for lower principal quantum numbers, we are not too far away from the regime where the dynamics could be visible within the lifetime of the central Rydberg atom. A comparison of the interaction coefficients with the inverse lifetime (brown line) is shown below.

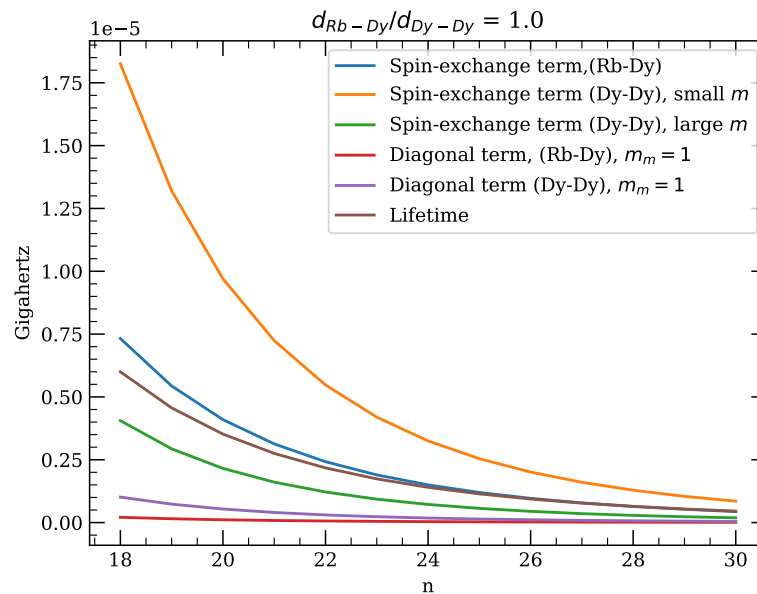


Figure 2: Lifetimes vs. Matrix elements of the magnetic dipolar interaction. The distance is assumed to be five times the radius at which the radial wave function of the electron of the central Rydberg atom is maximal.

Due to the proportionality of the interaction to  $r^{-3}$ , putting the atoms closer together could obviously make the interactions stronger, possibly sufficiently strong for the system to be interesting. In that case, the interaction cannot be

### 3 Multiple Circular Rydberg Atoms

#### 3.1 The proposed system

Idea: Use electric dipolar interactions between different circular Rydberg atoms to build quantum simulator. One Rydberg atom (in the following called the central Rydberg atom, although on principle any geometry is possible) has a higher principal quantum number (e.g.  $n = 70$ ) than the other circular Rydberg atoms (called the bath atoms, e.g. with  $n' = 35$ ). Initially, the bath atoms are thought to be arranged in a ring around the central atom in the  $xy$ -plane.

A constant and homogeneous external electric and magnetic field are applied,  $\vec{E} = E\vec{e}_z$ ,  $\vec{B} = B\vec{e}_z$ . The fields are always parallel and thus define the quantisation axis (electric field mixes states with different  $n, l$ , but  $m$  is still a good quantum number). By lifting the degeneracy between the circular state and states with other quantum numbers  $l, m$ , this enhances the lifetime of the circular state (?).

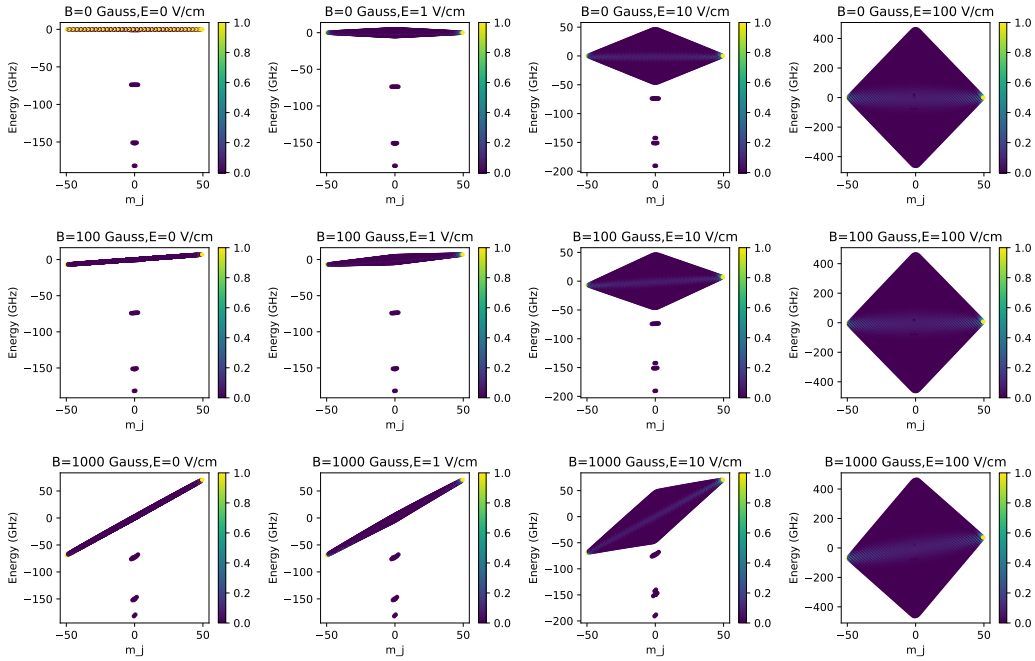


Figure 3: Exemplary Spectra of the Rydberg atom with principal quantum number  $n = 50$  in different electric and magnetic fields

The choice of  $n, n'$  has been made such that the spin exchange matrix elements for the central-bath interaction are approximately 10 times as large as those for the bath-bath interaction (at identical distance).

The circular Rydberg atoms interact predominantly through electric dipole-dipole interaction, magnetic dipolar interactions are approx. 7 or more orders of magnitude smaller (see the Data section for some numbers).



Electric dipole-dipole Interaction:

$$\hat{V}_{dd} = \frac{1}{4\pi\epsilon_0} \sum_{q,q'=-1}^1 v_{qq'}^{geom.}(\vec{r}) \hat{d}_q \hat{d}_{q'}, \quad (3.1)$$

where the electric dipole operator  $\hat{d}_q$  acts on one particle,  $\hat{d}_{q'}$  on the other. We have for  $\vec{r} = (r, \vartheta, \varphi)$ , the difference vector of the positions of the two atoms,

$$v_{zz}(\vec{r}) = \frac{1 - 3 \cos^2 \vartheta}{r^3},$$

$$v_{+-}(\vec{r}) = v_{-+}(\vec{r}) = \frac{1}{2} \cdot \frac{1 - 3 \cos^2 \vartheta}{r^3},$$

and the other contributions vanish because for the proposed setup, the dipolar interaction conserves  $d_z$ .

The Hamiltonian of this system is given by

$$\hat{H} = \sum_k \hat{H}_{1B}^{(k)} + \sum_{k,k'} V_{dd}^{(kk')}, \quad (3.2)$$

where  $\hat{H}_{1B}^{(k)}$  is the one-body Hamiltonian of the  $k^{\text{th}}$  atom, and  $V_{dd}^{(kk')}$  is the dipole-dipole interaction between particles  $k$  and  $k'$ .

The one-body Hamiltonian is the Hamiltonian of an electron in a hydrogen-like potential (very good approximation for circular Rydberg states) plus the influence of the external electric and magnetic fields. The circular state experiences a linear Zeeman shift from the magnetic field and a second-order Stark shift quadratic in  $E$  from the electric field. The *pairinteraction* library is used for computations.

We select two states for each atom to which we limit the dynamics. These are the circular states  $|n, C\rangle$  and  $|n-1, C\rangle$  respectively  $|n', C\rangle$  and  $|n'-1, C\rangle$ . Technically, these are not really the circular states anymore because the external electric field mixes them with other states.

The dipole-dipole interaction allows for the exchange of one unit of orbital angular momentum ( $|n, C; n'-1, C\rangle \leftrightarrow |n-1, C; n', C\rangle$ ). To make this exchange between the central and the bath atoms resonant, a microwave field is applied to dress the states [Mey21, Chapter 1.3]. For each atom, this adds to the Hamiltonian of the two-level system a term  $-\hat{d} \cdot \vec{E}_{mw}$ . Near resonance, the rotating wave approximation is a good approximation.

It provides us with two new states, the dressed states

$$|\downarrow\rangle = \cos \vartheta |n-1, C\rangle - \sin \vartheta |n, C\rangle,$$

$$|\uparrow\rangle = \sin \vartheta |n-1, C\rangle + \cos \vartheta |n, C\rangle,$$

where with the Rabi frequency  $\Omega_R = \hbar E_{mw} d_x$  (assuming  $\vec{E}_{mw} = E_{mw} \vec{e}_x$ ) and the detuning  $\Delta = (E_{|n,C\rangle} - E_{|n-1,C\rangle}) - \omega$   $\tan \frac{\vartheta}{2} = -\frac{\Omega_R}{\Delta}$ , and  $-\frac{\pi}{4}$  if  $\Delta = 0$ .

Note that the direction of the microwave field plays a role here because any z-component just adds

some terms to the diagonal terms of the Hamiltonian in the original representation.

The dressed states  $|1\rangle, |2\rangle$  are our effective spin states  $|\uparrow\rangle, |\downarrow\rangle$ . We now proceed to expressing the Hamiltonian in terms of the effective spin states. In the basis  $(|\downarrow\rangle, |\uparrow\rangle)$  the one-body Hamiltonian is diagonal,

$$\hat{H}_{1B} = \begin{pmatrix} \frac{E_{|n,C\rangle} + E_{|n-1,C\rangle}}{2} - \hbar\Omega/2 & 0 \\ 0 & \frac{E_{|n,C\rangle} + E_{|n-1,C\rangle}}{2} + \hbar\Omega/2 \end{pmatrix}, \quad (3.3)$$

where  $\Omega = \sqrt{\Omega_R^2 + \Delta^2}$ .

The dipole-dipole interaction can be expressed in terms of the dressed states. Changing from the two-two-level-system basis

$$(|n_k - 1, C; n_{k'} - 1, C\rangle, |n_k - 1, C; n_{k'}, C\rangle, |n_k, C; n_{k'} - 1, C\rangle, |n_k, C; n_{k'}, C\rangle) \quad (3.4)$$

to the dressed-state basis

$$(|\downarrow_k, \downarrow_{k'}\rangle, |\downarrow_k, \uparrow_{k'}\rangle, |\uparrow_k, \downarrow_{k'}\rangle, |\uparrow_k, \uparrow_{k'}\rangle) \quad (3.5)$$

with the basis change matrix (from effective spin basis to circular states basis)

$$B = \begin{pmatrix} \cos \vartheta_k \cos \vartheta_{k'} & \cos \vartheta_k \sin \vartheta_{k'} & \sin \vartheta_k \cos \vartheta_{k'} & \sin \vartheta_k \sin \vartheta_{k'} \\ -\cos \vartheta_k \sin \vartheta_{k'} & \cos \vartheta_k \cos \vartheta_{k'} & -\sin \vartheta_k \sin \vartheta_{k'} & \sin \vartheta_k \cos \vartheta_{k'} \\ -\sin \vartheta_k \cos \vartheta_{k'} & -\sin \vartheta_k \sin \vartheta_{k'} & \cos \vartheta_k \cos \vartheta_{k'} & \cos \vartheta_k \sin \vartheta_{k'} \\ \sin \vartheta_k \sin \vartheta_{k'} & -\sin \vartheta_k \cos \vartheta_{k'} & -\cos \vartheta_k \sin \vartheta_{k'} & \cos \vartheta_k \cos \vartheta_{k'} \end{pmatrix}.$$

We define

$$\begin{aligned} d_z^{(k,n-1)} &= \langle n_k - 1, C | \hat{d}_z^{(k)} | n_k - 1, C \rangle \\ d_z^{(k,n)} &= \langle n_k, C | \hat{d}_z^{(k)} | n_k, C \rangle \\ d_-^{(k)} &= \langle n_k - 1, C | \hat{d}_-^{(k)} | n_k, C \rangle \\ d_+^{(k)} &= \langle n_k, C | \hat{d}_+^{(k)} | n_k - 1, C \rangle \end{aligned}$$

In the circular states basis (3.4), the dipole-dipole interaction is represented by the matrix

$$V_{dd,C}^{(kk')} = \frac{1}{4\pi\epsilon_0} \frac{1 - 3\cos^2\vartheta}{r^3} \begin{pmatrix} d_z^{(k,n-1)} d_z^{(k',n'-1)} & & 0 & 0 \\ 0 & d_z^{(k,n)} d_z^{(k',n'-1)} & d_-^{(k)} d_+^{(k')} & 0 \\ 0 & d_+^{(k)} d_-^{(k')} & d_z^{(k,n-1)} d_z^{(k',n')} & 0 \\ 0 & 0 & 0 & d_z^{(k,n)} d_z^{(k',n')} \end{pmatrix}.$$

The *pairinteraction* library is used to calculate the matrix elements.

The representation of the dipole-dipole interaction in the effective spin basis (3.5) is therefore

given by

$$V_{dd,spins}^{(kk')} = B^{-1}V_{dd,C}^{(kk')}B. \quad (3.6)$$

Non- $S_z$ -conserving terms appear because the microwave field breaks the z-symmetry.

### 3.2 The effective Hamiltonian

Our goal is to rewrite the interaction in terms of a system of spin-1/2 variables with interactions between pairs of spins. To do so, we bring the interaction in the form

$$\hat{V}^{kk'} = \sum_{q,q' \in \{z,-,+\}} J_{qq'}^{kk'} \hat{S}_q^{(k)} \hat{S}_{q'}^{(k')}.$$

In the basis (3.5), this is represented by the matrix

$$V_{spins}^{kk'} = \begin{pmatrix} \frac{1}{4}J_{zz} & -\frac{1}{2}J_{z-} & -\frac{1}{2}J_{-z} & J_{--} \\ -\frac{1}{2}J_{z+} & -\frac{1}{4}J_{zz} & J_{-+} & \frac{1}{2}J_{-z} \\ -\frac{1}{2}J_{+z} & J_{+-} & -\frac{1}{4}J_{zz} & \frac{1}{2}J_{z-} \\ J_{++} & \frac{1}{2}J_{+z} & \frac{1}{2}J_{z+} & \frac{1}{4}J_{zz} \end{pmatrix}. \quad (3.7)$$

Comparison with some exemplary interactions in the system of the two Rydberg atoms (3.6) shows that this interaction does not always precisely have this form. There are some terms that can easily be accounted for by other reasonable terms and some terms for which it is yet unclear how they can be explained in the spin-1/2 picture. Consider the diagonal terms of (3.6) first. In order to bring the diagonal terms into the form of the diagonal terms of (3.7), we introduce two effective magnetic fields  $B_k \vec{e}_z, B_{k'} \vec{e}_z$  that act on the spins  $k, k'$  respectively. These add to the Hamiltonian of the system of two spins a term

$$\hat{H}_{add} = B_k \hat{S}_z^{(k)} + B_{k'} \hat{S}_z^{(k')} + E_0 \hat{I}, \quad (3.8)$$

where  $\hat{I}$  is the identity operator. In the basis (3.5), the additional term (3.8) is given by

$$H_{add} = B_k \begin{pmatrix} -1 & & & \\ & -1 & & \\ & & 1 & \\ & & & 1 \end{pmatrix} + B_{k'} \begin{pmatrix} -1 & & & \\ & 1 & & \\ & & -1 & \\ & & & 1 \end{pmatrix} + E_0 \begin{pmatrix} 1 & & & \\ & 1 & & \\ & & 1 & \\ & & & 1 \end{pmatrix}.$$

Together with the diagonal of (3.7), we have four linearly independent diagonal matrices that account for the diagonal of (3.6). Given an interaction (3.6), the coefficients  $J_{zz}, B_k, B_{k'}, E_0$  are therefore always uniquely determined and all needed to rewrite the interaction between the two Rydberg atoms in terms of the spin-spin Hamiltonian.

The effective B-fields are easy to understand, but I have not yet thought about if the sum of all the constant energy shifts from the two-body interactions cause one shift to the whole diagonal of

the full Hamiltonian or if different diagonal entries are shifted by different values.

The effective B-fields make it challenging to find out when the resonance condition for the spin exchange is met, since they introduce an additional energy difference between the effective spin-up and -down states that depends on all the tunable parameters  $E, B$  and the microwave field(s).

Let us now consider the off-diagonal entries of the interaction (3.6). Certain matrix elements must be (up to a change of sign) of the same magnitude in the spin-spin interaction. This, however, does not automatically seem to be fulfilled. I believe that this can be traced back to the fact that for the effective spin states, the expectation values  $\langle \downarrow_k | \hat{d}_z^{(k)} | \downarrow_k \rangle$  and  $\langle \uparrow_k | \hat{d}_z^{(k)} | \uparrow_k \rangle$  do not necessarily have the same absolute value. From looking at a few examples, this asymmetry seems to be small (maybe one percent of the absolute value of these), and potentially the asymmetry of both the value associated with  $J_{z-}$  and  $J_{z+}$  can be obtained by rescaling the eigenvalues of  $\hat{S}_z$  by the same factor. I looked at one example where that would have worked.

Translating the one-body Hamiltonian (3.3) into the spin-1/2 picture is straightforward and adds contributions  $\Omega_k$  to the effective B-field  $B_k \vec{e}_k$ .

### 3.3 Simulating the dynamics

Using the one- and two-body Hamiltonians that were derived in the previous sections, we can explicitly find the full Hamiltonian of the physical system of the circular Rydberg atoms. Exact (numerical) diagonalisation provides a direct way to simulate its dynamics. We determine and plot the expectation values  $\langle \hat{S}_z^{(k)} \rangle$  as well as  $\sum_k \langle \hat{S}_z^{(k)} \rangle$  as functions of time.

We therefore use that the time evolution of any initial state  $|\Psi_0\rangle$  of our system is given by the Schrödinger equation as

$$|\Psi(t)\rangle = \sum_j e^{-iE_j t/\hbar} \langle \psi_j | \Psi_0 \rangle |\psi_j\rangle,$$

where  $E_j$  are the eigenvalues of our Hamiltonian and  $|\psi_j\rangle$  the corresponding eigenvectors.

The time evolution of  $\langle \hat{S}_z^{(k)} \rangle$  therefore depends on the given initial state as well as the pairwise *differences* of the eigenvalues,

$$\langle \hat{S}_z^{(k)} \rangle(t) = \sum_{j,l} e^{-i(E_j - E_l)t/\hbar} \langle \psi_j | \Psi_0 \rangle \langle \Psi_0 | \psi_l \rangle \langle \psi_l | \hat{S}_z^{(k)} | \psi_j \rangle.$$

Similarly, the time evolution of the expectation values of the magnetic quantum number  $\langle \hat{m}^{(k)} \rangle$  can be calculated as functions of time.

Some plots visualising both will be added soon (I am not sure if I have them on my own laptop but I will add them tomorrow morning at latest).

There are a number of interesting questions that could be asked in relation to this time evolution. For example, its dependence on the geometry could be investigated. To do so, I first introduced an angle by which the ring can be tilted, but more complex geometries could also easily be realised with my programme. Noise can be added to the initial state so that not all bath atoms have well-defined  $S_z$  in the initial state. The bath interactions can be switched on and off. The non-

$S_z$ -conserving terms can be switched on and off. I did a little bit of everything, but I have not systematically investigated anything (yet). The reasons for that are mainly that I did not know what parameter ranges to investigate and how to solve the problem that it is very hard to make the spin exchange resonant (so for my plots it is probably most of the time not really resonant, but that should be visible). Some example time evolutions are shown below. The subtitles explain what is the point of the plot, and contain the initial state (where the first entry corresponds to atom 0, the second one to atom 1 etc., and atom 0 is the central atom surrounded by a ring of bath atoms).

blue is with bath, orange without

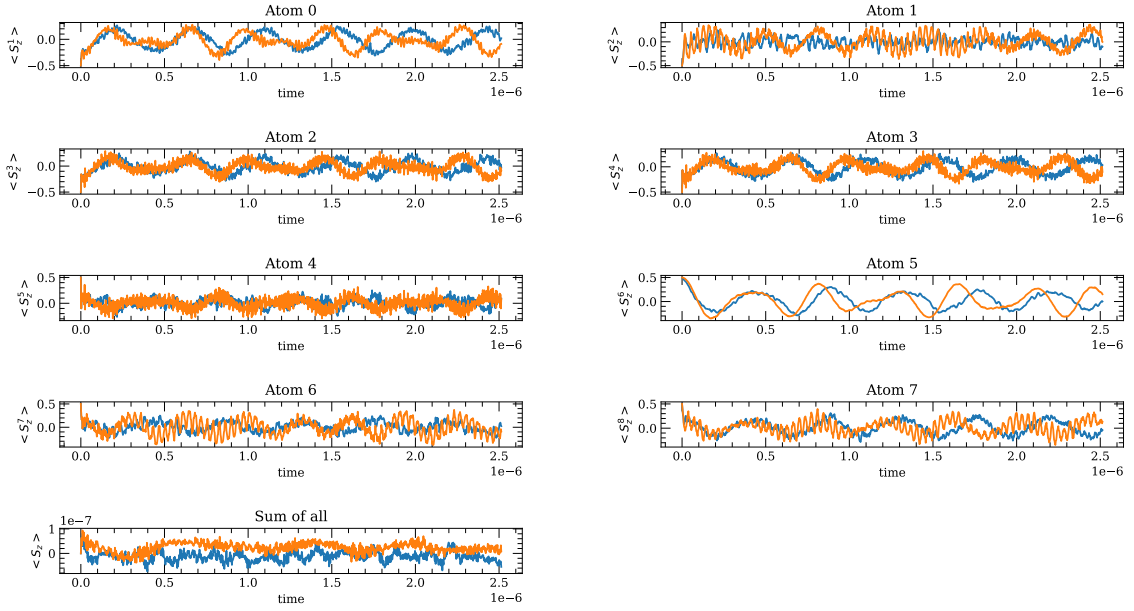


Figure 4: Switching on and off the bath interactions, initial state  $|\downarrow\downarrow\downarrow\downarrow\uparrow\uparrow\uparrow\uparrow\rangle$

blue is with bath, orange without

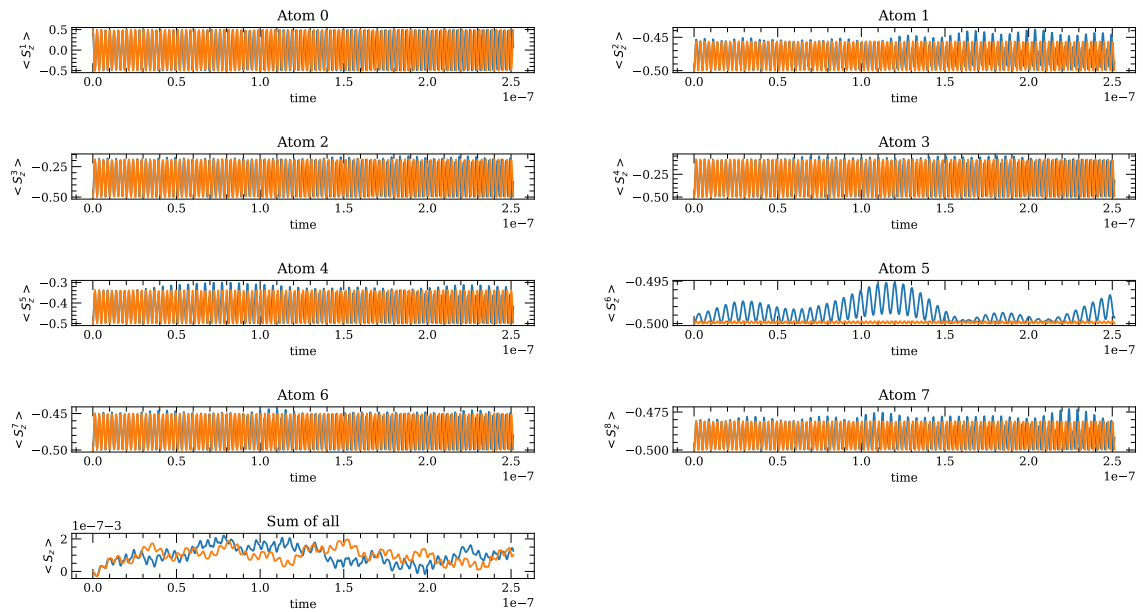


Figure 5: Switching on and off the bath interactions, initial state  $|\uparrow\downarrow\downarrow\downarrow\downarrow\downarrow\downarrow\downarrow\rangle$

blue is with bath, orange without

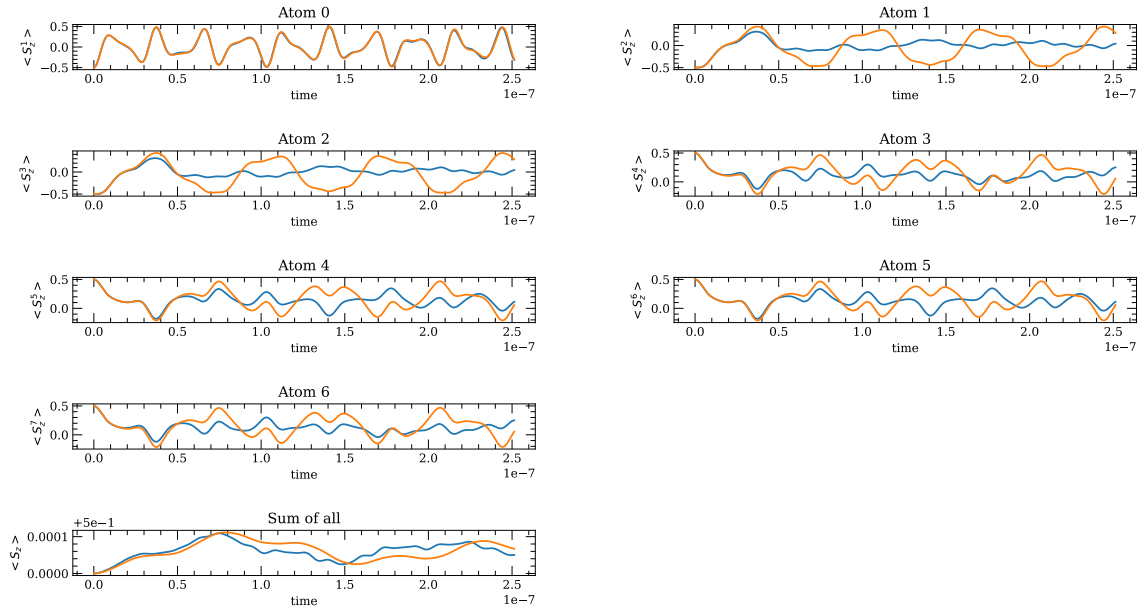


Figure 6: Switching on and off the bath interactions, initial state  $|\downarrow\downarrow\downarrow\uparrow\uparrow\uparrow\uparrow\rangle$



blue is nonconserving  $S_z$ , orange conserving  $S_z$

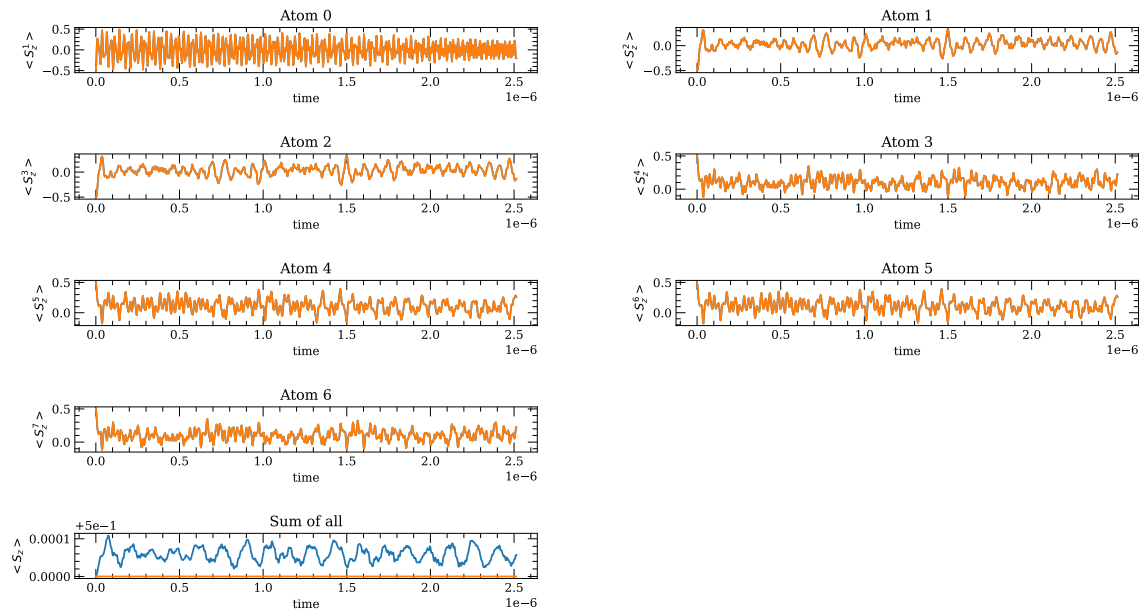


Figure 7: Switching on and off the non- $S_z$  conserving terms, initial state  $|\downarrow\downarrow\downarrow\uparrow\uparrow\uparrow\uparrow\rangle$

blue is nonconserving  $S_z$ , orange conserving  $S_z$

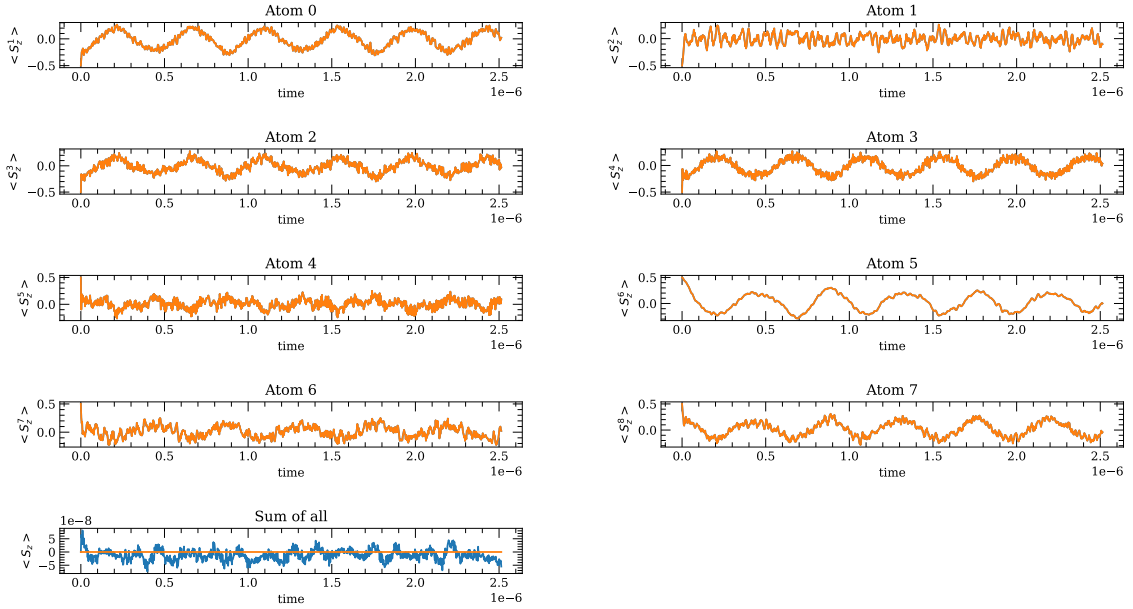


Figure 8: Switching on and off the non- $S_z$  conserving terms, initial state  $|\downarrow\downarrow\downarrow\downarrow\uparrow\uparrow\uparrow\uparrow\rangle$

### 3.4 Alternative states selection

#### 3.4.1 The system

This is meant to be easier (from a calculational point of view). Instead of dressing two neighbouring circular states with a microwave field, we select the circular state and one with magnetic quantum number  $m$  being one lower than the circular state (or more correctly their correspondents after

switching on the external fields) and adjust their transition frequencies with the external fields until they are equal for both the central and the bath atom (similar to the magnetic atoms). This seems to be very easy because apparently this difference does, for one of the three Zeeman-split states with  $m = m_{\max} - 1$ , the energy difference to the circular state seems very very very similar for all  $n$ , see Figure 9.

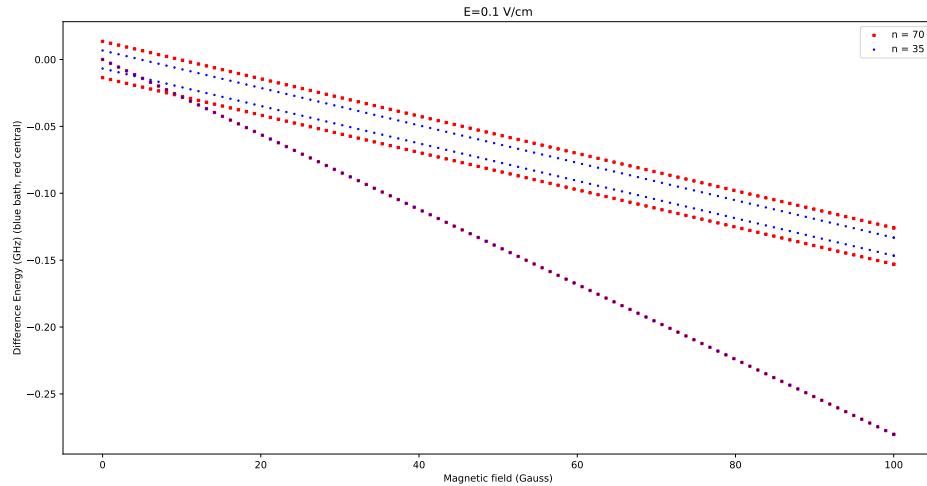


Figure 9: Energy differences of the states with  $m_j = n - 2$  to the circular state in  $GHz$ .

Apparently one of these has an almost equal transition frequency for both  $n' = 35$  and  $n = 70$ . I investigated this for various combinations of  $n, n'$  and up to very high electric fields ( $E = 1000V/cm$ ), and this observation holds for all values I checked. If this is indeed the case, it makes this pair of states a very useful candidate for our two-level system.

The interaction is given by the electric dipolar interaction.

This eliminates the need of a microwave field and therefore gets rid of the following problems:

- Change in transition frequency which is non-predictable, made the choice of suitable parameters very difficult
- non- $S_z$  conserving terms
- Asymmetry of interaction

Our effective spin-up state is the eigenstate of the Hamiltonian of the electron in the external electric and magnetic field that has the largest contribution from the circular state. The effective spin-down state is one of the three eigenstates with  $m = n - 2$  (which is one less than the circular state). For some exemplary values of  $E, B$ , the decomposition of these states into the states with quantum numbers  $n, l, j, m$  is shown below.

```
* Electric field along Z axis set to: 1 V/cm
* Magnetic field along Z axis set to: 34 Gauss
2.236484353799142 48.5 +0.7069521257138576 |Rb, 50 48_97/2, mj=97/2> -0.7036803094316499 |Rb, 50 49_99/2, mj=97/2> +0.071082
44556031901 |Rb, 50 49_97/2, mj=97/2>
2.2852294442575385 48.5 -0.9949366763222188 |Rb, 50 49_97/2, mj=97/2> -0.10050378156515445 |Rb, 50 49_99/2, mj=97/2>
2.4294102217254476 48.5 +0.7072614028410276 |Rb, 50 48_97/2, mj=97/2> +0.7033725982786657 |Rb, 50 49_99/2, mj=97/2> -0.07105
13620000387 |Rb, 50 49_97/2, mj=97/2>
```

Figure 10: Decomposition of the eigenstates

Moreover, the down-state has no well-defined quantum numbers  $n, l$  anymore and we choose one of the three states with  $m = n - 2$  so that the transition frequencies in both kinds of atoms match as can be seen in Figure 9.

The interaction is given by (3.1), the one-body Hamiltonian is that of the electron in the potential of the nucleus and in the external electric and magnetic field. The full Hamiltonian is (3.2), and deriving the effective Hamiltonian is straightforward. By comparison with (3.6), it is obvious that there are no terms  $J_{+z}, J_{-z}, J_{z+}, J_{z-}, J_{++}, J_{--}$ . The additional effective  $B$ -field and energy shift from (3.8) also appear.

The dipole moments  $\langle n', l', j', m' | \hat{d} | n, l, j, m \rangle$  and the products of the weights of these states in the decomposition of the eigenstates of the Hamiltonian are shown below. We observe that the contributions come from states with  $|n' - n| \geq 1$ .

```
states: f, i: n, l, j, m
70 69 69.5 69.5
70 69 68.5 68.5
Dipole Moments
0.0
product of weights f, i
0.9959963716351007
states: f, i: n, l, j, m
70 69 69.5 69.5
70 69 69.5 68.5
Dipole Moments
-0.0
product of weights f, i
0.08478484397935748
states: f, i: n, l, j, m
71 70 70.5 69.5
70 69 68.5 68.5
Dipole Moments
0.0
product of weights f, i
0.02809907987944291
states: f, i: n, l, j, m
71 70 70.5 69.5
70 69 69.5 68.5
Dipole Moments
4.416412111973048
product of weights f, i
0.0023919525927900585
states: f, i: n, l, j, m
71 70 69.5 69.5
70 69 68.5 68.5
Dipole Moments
4.447842486906898
product of weights f, i
-0.002374805588677882
```

Figure 11: Contributions to the dipole moments  $\langle n', l', j', m' | \hat{d} | n, l, j, m \rangle$ , external fields are  $E = 1V/cm, B = 1Gauss$ .

### 3.4.2 The interaction coefficients

I plotted the dependence of the coefficients  $J_{+-}$  and  $J_{zz}$  as a function of the external fields. Some plots can be seen below. For all plotted coefficients we take  $\frac{(1-3\cos^2\vartheta)}{r^3} = 1\mu\text{m}^{-3}$ .

For all considered values of the external fields (which are  $0 \leq B \leq 1000 \text{ Gauss}$  and  $0 \leq E \leq 1000 \text{ V/cm}$ ), the exchange-interaction coefficients are several orders of magnitudes smaller than the diagonal terms. Some exemplary plots are shown below.

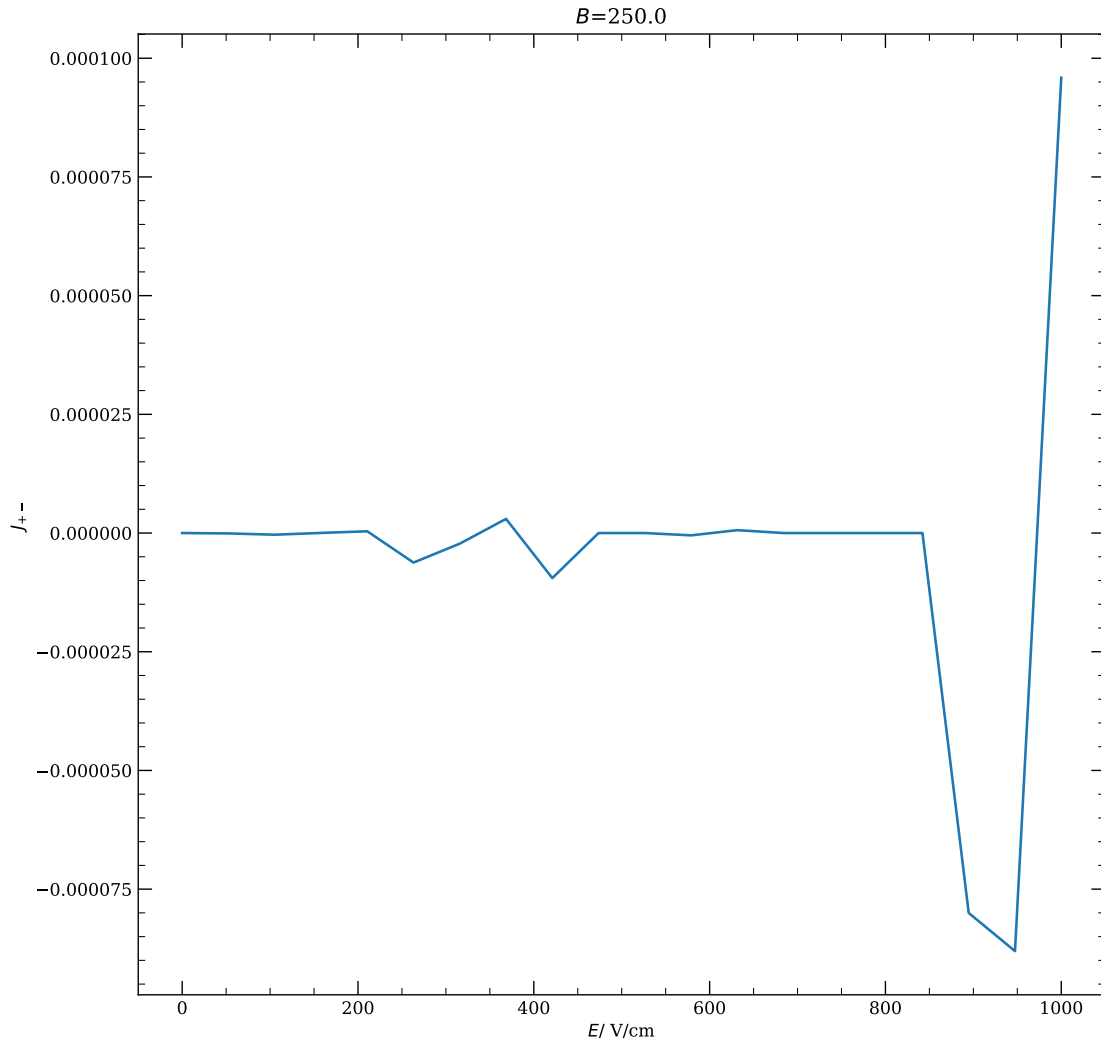


Figure 12: The coefficient  $J_{+-}$  in GHz between the central and the bath atom as a function of the electric field  $E$  at low magnetic field  $B \approx 6.3 \text{ V/cm}$

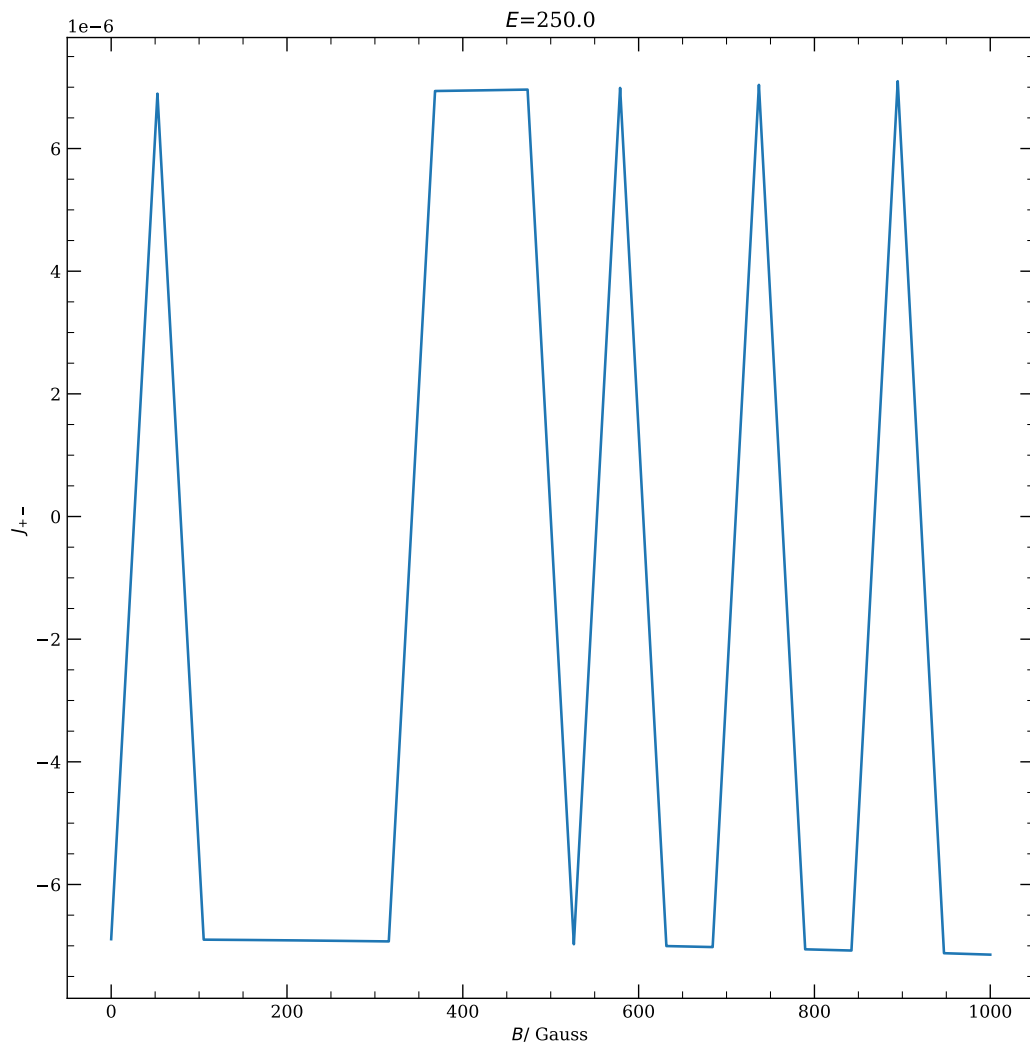


Figure 13: The coefficient  $J_{+-}$  in GHz between the central and the bath atom as a function of the magnetic field  $B$  at electric field  $E = 250V/cm$

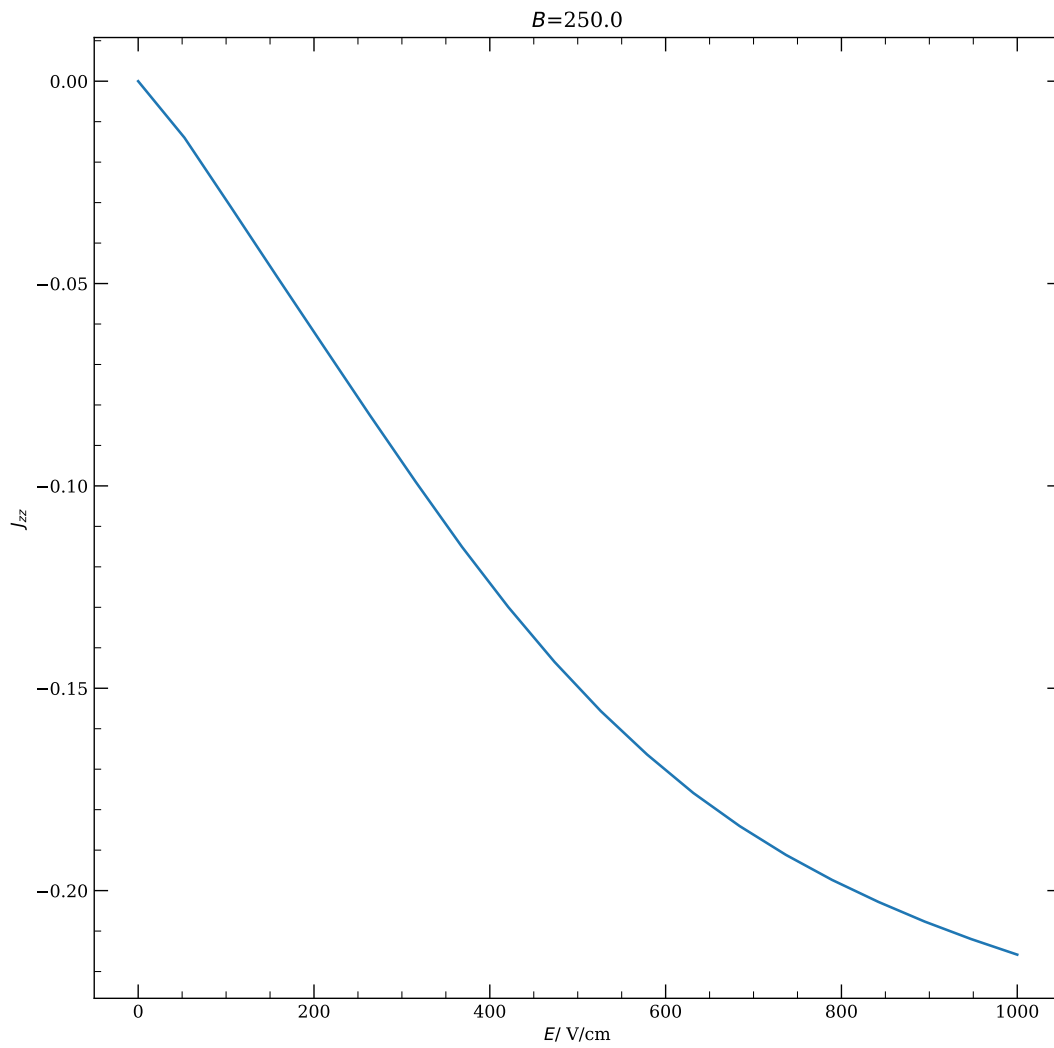


Figure 14: The coefficient  $J_{zz}$  in GHz between the central and the bath atom as a function of the electric field  $E$  at low magnetic field  $B \approx 6.3 \text{ V/cm}$

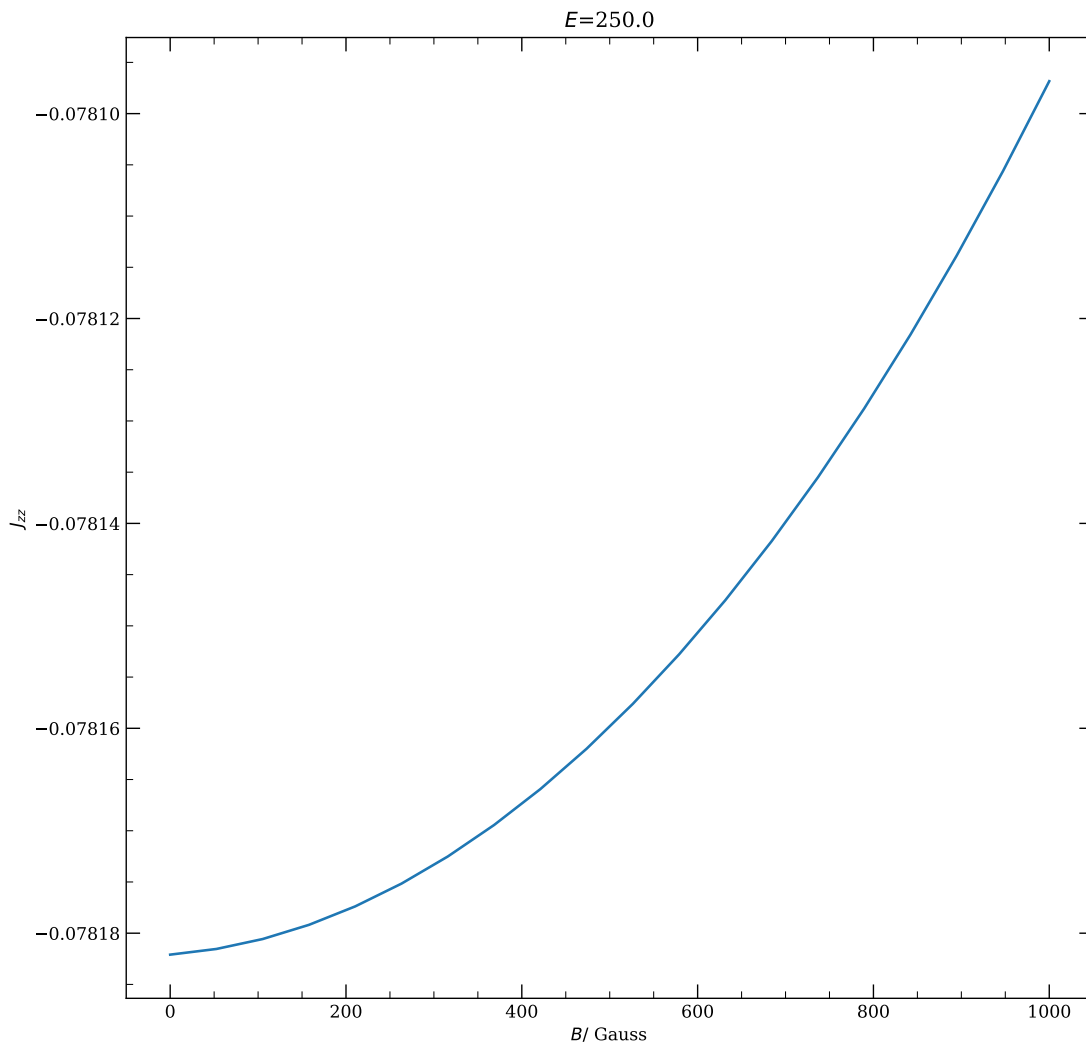


Figure 15: The coefficient  $J_{zz}$  in GHz between the central and the bath atom as a function of the magnetic field  $B$  at electric field  $E = 250V/cm$



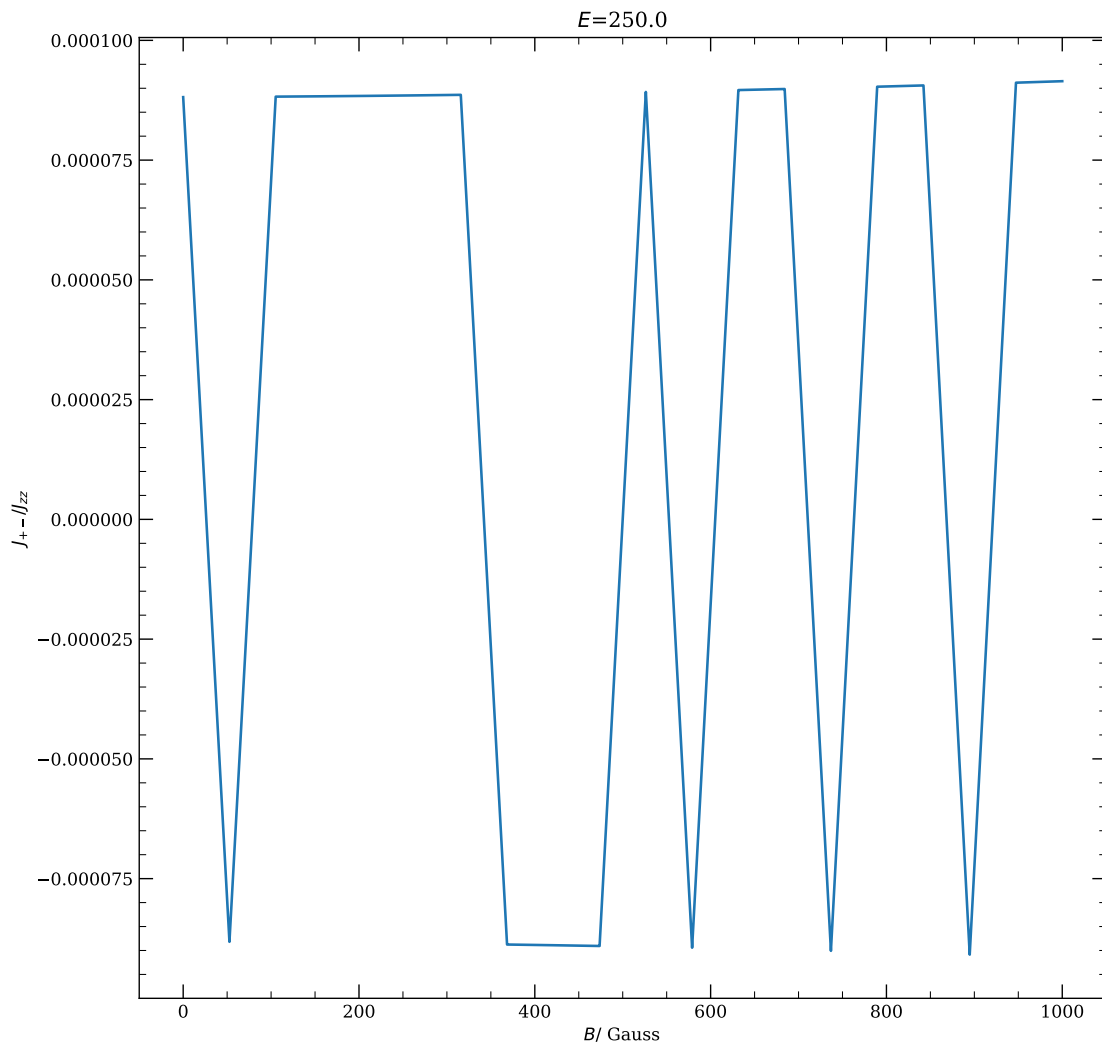


Figure 16: The ratio of the coefficients  $J_{+-}/J_{zz}$  in GHz between the central and the bath atom as a function of the magnetic field  $E$  at electric field  $E = 250 \text{ V/cm}$

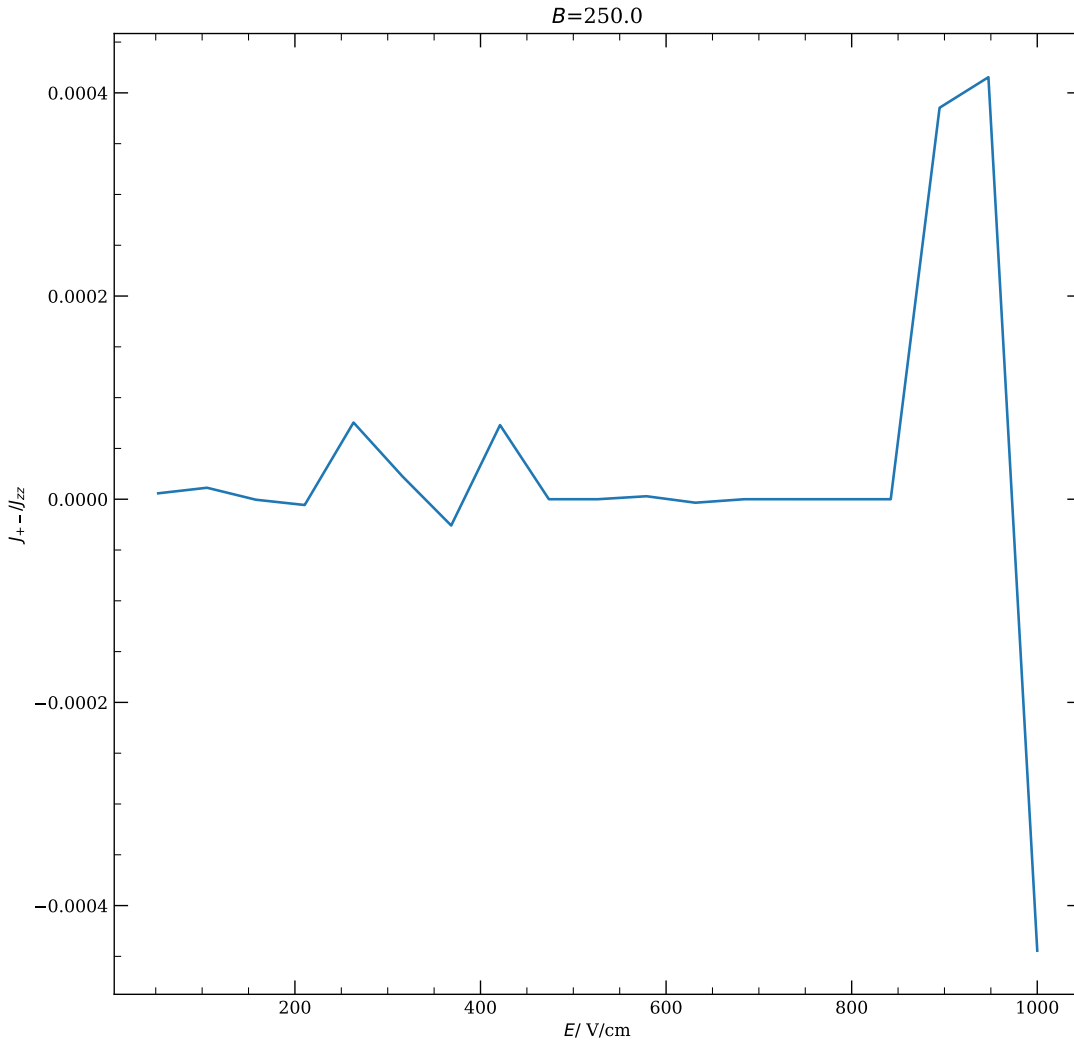


Figure 17: The ratio of the coefficients  $J_{+-}/J_{zz}$  in GHz between the central and the bath atom as a function of the electric field  $E$  at magnetic field  $B = 250$  Gauss

## 4 Data

### 4.1 Different small considerations

Lifetimes of different Rydberg states calculated with the ARC library using Jacek's program.

$n$	34	35	40	50	60	69	70	80	90	100
$\tau_n/ms$	4.1	4.8	9.2	24.5	45.0	65.1	67.4	91.4	117.5	146.2

Table 2: Lifetimes at  $T = 1K$

No possibility to enter  $m_j$  into lifetime code.

Some orders of magnitude for the dipolar interaction matrix elements.

Diagonal (central - bath) (up-up): 0.010512262620719248	Diagonal (central - bath) (up-up): 3.010256381427342e-09
Diagonal (central - bath) (up-down): 0.010065014758629967	Diagonal (central - bath) (up-down): 2.924654094969778e-09
Diagonal (central - bath) (down-up): 0.010273712265573793	Diagonal (central - bath) (down-up): 2.9668546304849244e-09
Diagonal (central - bath) (down-down): 0.00983661361114692	Diagonal (central - bath) (down-down): 2.882486554222829e-09
Off-diagonal (central - bath): -0.248976902917912	Off-diagonal (central - bath): 2.7531221463226643e-09
Diagonal (bath - bath) (up-up): 0.0013368471826878997	Diagonal (bath - bath) (up-up): 5.121870619375573e-10
Diagonal (bath - bath) (up-down): 0.0012799705552700496	Diagonal (bath - bath) (up-down): 4.976220621367603e-10
Diagonal (bath - bath) (down-up): 0.0012799705552700498	Diagonal (bath - bath) (down-up): 4.976220621367603e-10
Diagonal (bath - bath) (down-down): 0.0012255137637080264	Diagonal (bath - bath) (down-down): 4.834712454244521e-10
Off-diagonal (bath - bath): -0.02208992762053661	Off-diagonal (bath - bath): 4.5117876552364727e-10
Ratio diagonal central-bath / bath-bath: 11.271060149895765	Ratio diagonal central-bath / bath-bath: 6.102064983327251

Matrix elements for the electric dipole-dipole interaction,  $n = 70, n' = 35$ , where  $(r, \vartheta) = (5\mu m, \pi/2)$ .

Matrix elements for the magnetic dipole-dipole interaction,  $n = 70, n' = 35$ , where  $(r, \vartheta) = (5\mu m, \pi/2)$ .

The radial parts of the circular wave functions:

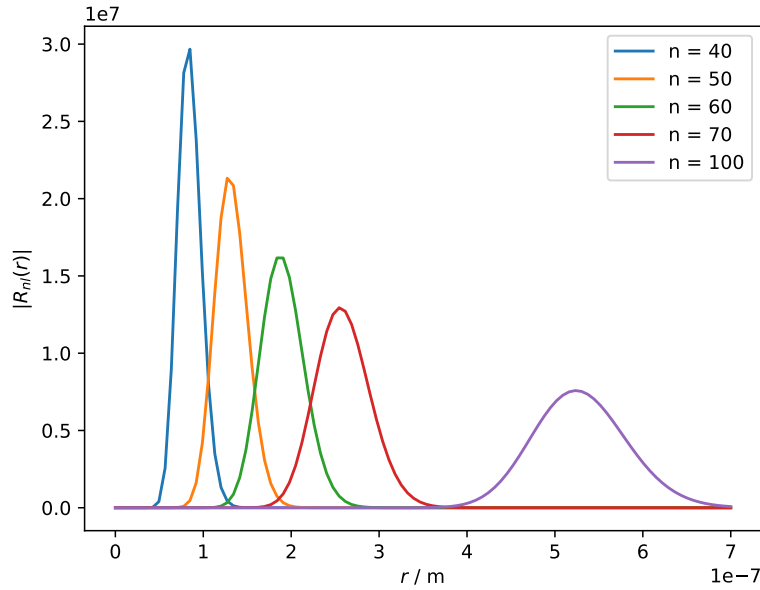


Figure 18: Radial wavefunction sfor circular states with different principal quantum numbers

To answer the question how many bath atoms with  $n_{bath} = 35$  can be placed on a ring with radius  $5\mu m$  where  $r_{35}$  is the radius for which the radial wavefunction has a maximum, I calculated the distance between equidistantly distributed atoms on this ring. The very low values are apparently nonsense. I added a line representing  $r = 10r_{35}$  which is a rough barrier above which I assume that the interaction can be considered to be represented very well by the dipole-dipole interaction.

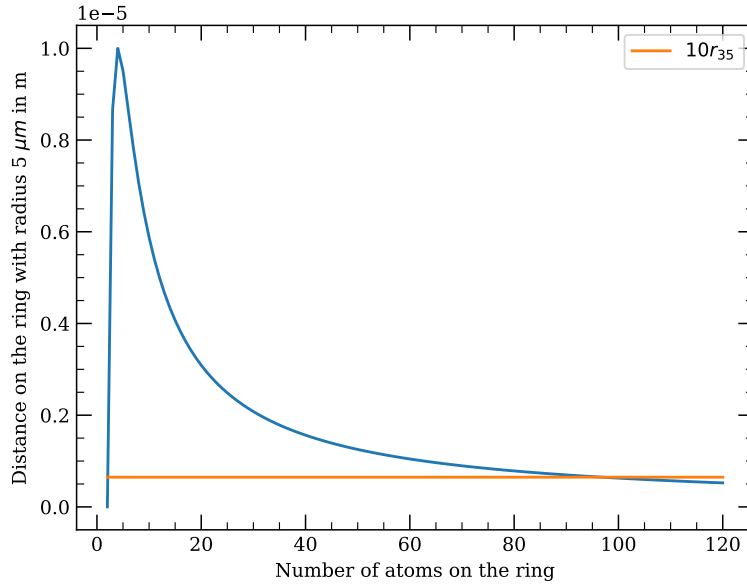


Figure 19: Distances of atoms on the ring as a function of the number of equidistributed atoms

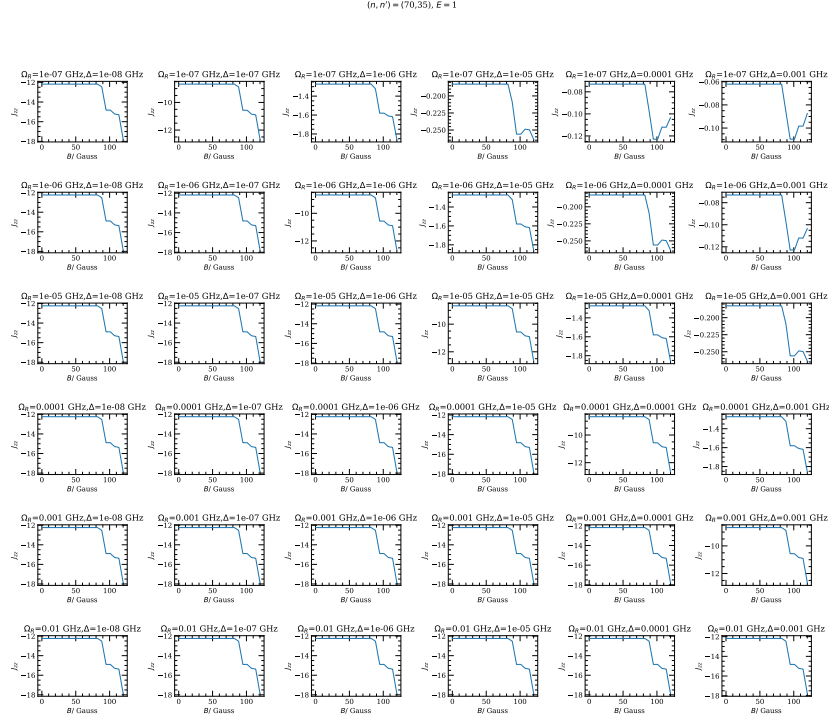
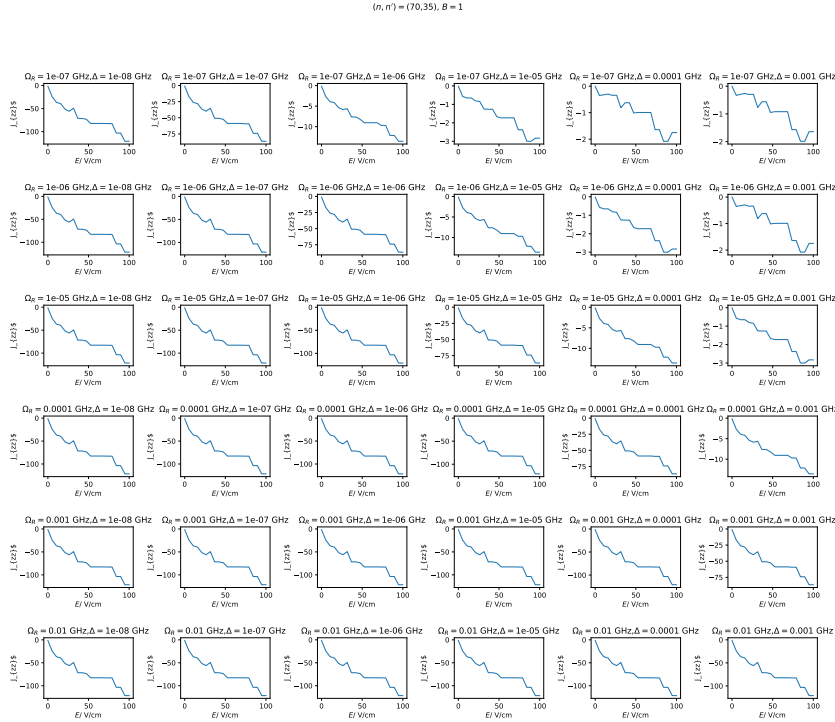
Potentially other considerations are relevant for an experimental realisation, e.g. how close can the tweezers be put together, but I don't really know much about that.

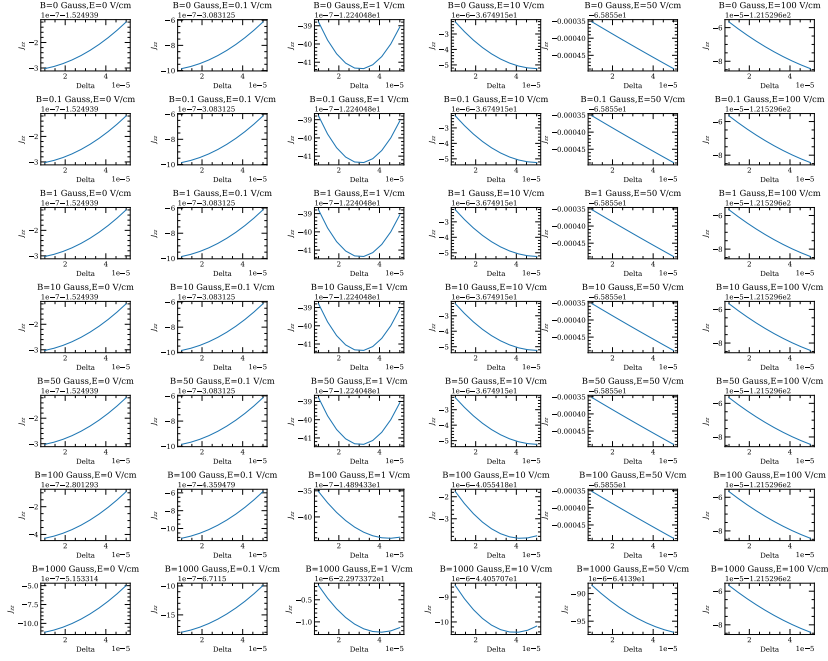
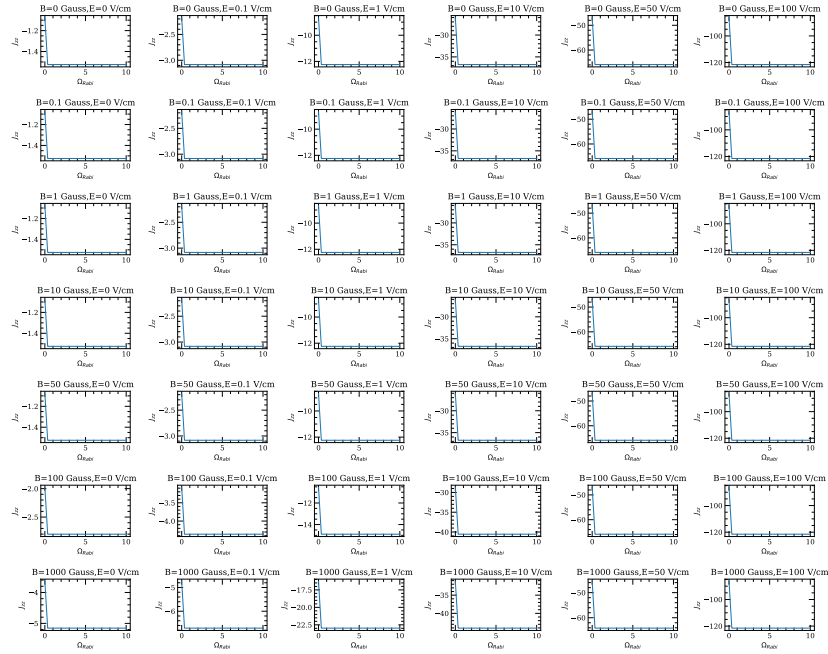
I thought about the question if the non- $\sum_k m_k$  conserving terms could maybe vanish not because of a conservation law (which I think is broken here), but because they are too well-separated in the Hamiltonian. However, it does not look as if that were the case.

## 4.2 Dependence of $J$ 's on various control parameters for the system using only circular states

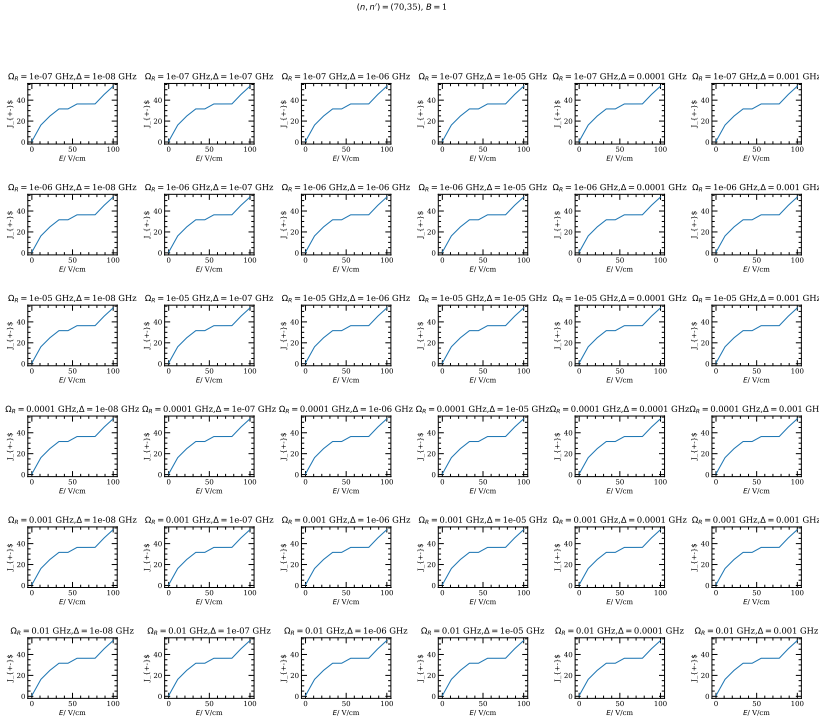
In the following, there are some plots that show the dependence of various interaction coefficients of the dipole-dipole interaction between the central Rydberg atom and one bath atom in the spin-1/2 representation on different control parameters. The parameters that can be varied are  $E, B$ , the detunings  $\Delta_k, \Delta_{k'}$  and the Rabi frequencies  $\Omega_R$ . I assumed equal detuning and Rabi frequency for both atoms, but it might in fact be more interesting and relevant to vary these independently.

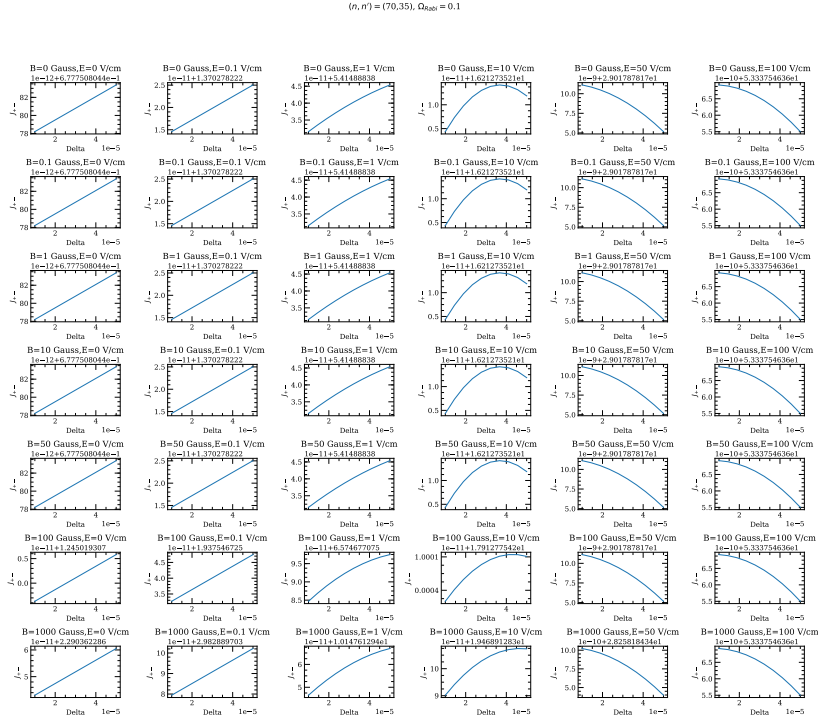
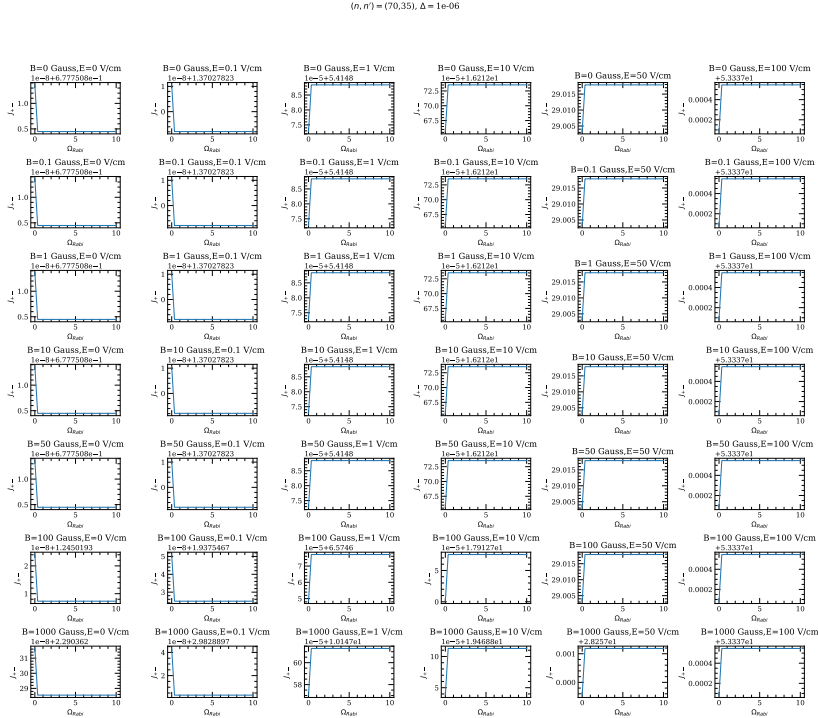
There is some systematic in how I arranged the plots (first one varies  $B$ , second varies  $E$ , third  $\Delta$ , last  $\Omega_R$ ). All  $J$ s are in  $\text{GHz}$ .

4.2.1  $J_{zz}$ 

 Figure 20:  $J_{zz}$  as a function of  $B$  for  $E = 1V/cm$  and different combinations of  $\Delta, \Omega_R$ 

 Figure 21:  $J_{zz}$  as a function of  $E$  for  $B = 1Gauss$  and different combinations of  $\Delta, \Omega_R$

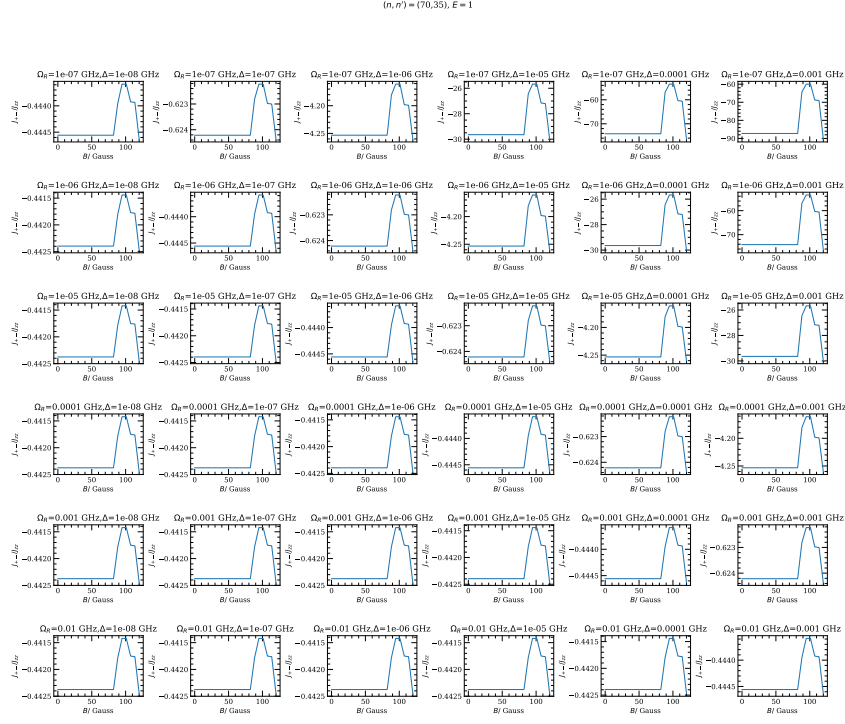
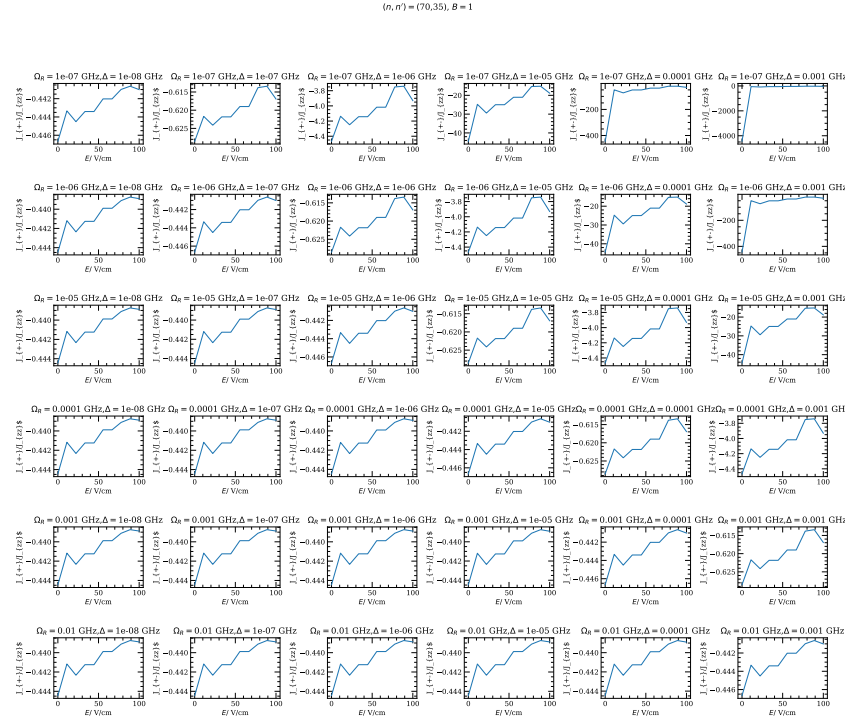
$(n, n') = (70, 35), Q_{\text{Rabi}} = 0.1$ 

 Figure 22:  $J_{zz}$  as a function of  $\Delta$  for  $\Omega_R = 0.1 \text{ GHz}$  and different combinations of  $E, B$ 
 $(n, n') = (70, 35), \Delta = 1e-06$ 

 Figure 23:  $J_{zz}$  as a function of  $\Omega_R$  for  $\Delta = 1 \text{ kHz}$  and different combinations of  $E, B$

4.2.2  $J_{+-}$  and  $J_{-+}$ 

 Figure 24:  $J_{+-}$  as a function of  $B$  for  $E = 1V/cm$  and different combinations of  $\Delta, \Omega_R$ 

 Figure 25:  $J_{+-}$  as a function of  $E$  for  $B = 1Gauss$  and different combinations of  $\Delta, \Omega_R$


 Figure 26:  $J_{+-}$  as a function of  $\Delta$  for  $\Omega_R = 0.1 \text{ GHz}$  and different combinations of  $E, B$ 

 Figure 27:  $J_{+-}$  as a function of  $\Omega_R$  for  $\Delta = 1 \text{ kHz}$  and different combinations of  $E, B$



4.2.3  $J_{+-}/J_{zz}$ 

 Figure 28:  $J_{+-}/J_{zz}$  as a function of  $B$  for  $E = 1V/cm$  and different combinations of  $\Delta, \Omega_R$ 

 Figure 29:  $J_{+-}/J_{zz}$  as a function of  $E$  for  $B = 1Gauss$  and different combinations of  $\Delta, \Omega_R$

$(n, n') = (70, 35), Q_{\text{Rabi}} = 0.1$

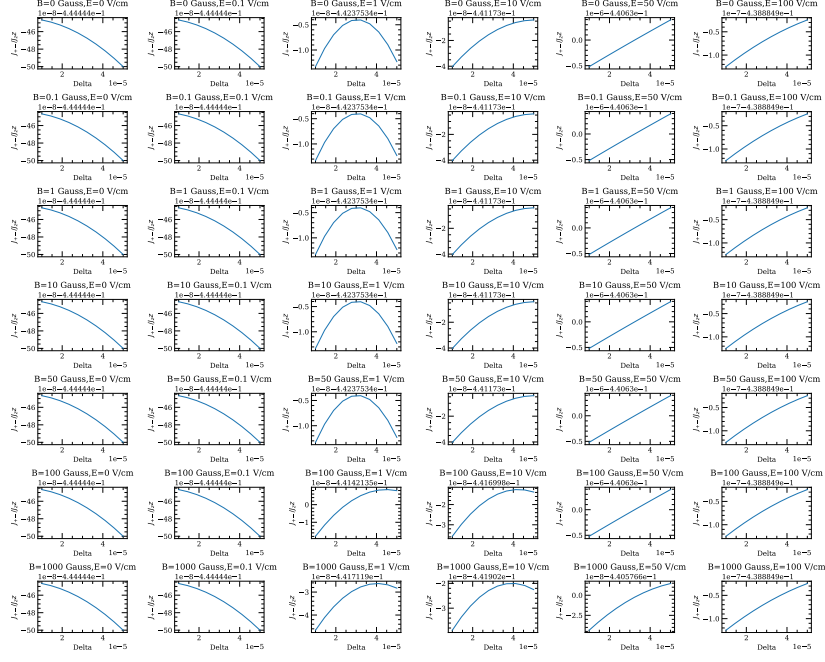


Figure 30:  $J_{+-}/J_{zz}$  as a function of  $\Delta$  for  $\Omega_R = 0.1\text{GHz}$  and different combinations of  $E, B$

$(n, n') = (70, 35), \Delta = 1e-06$

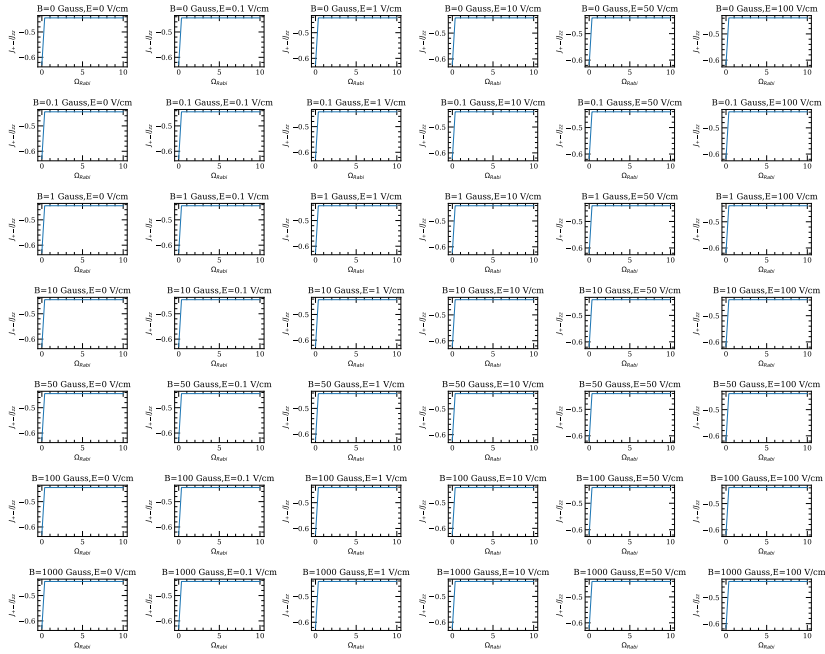
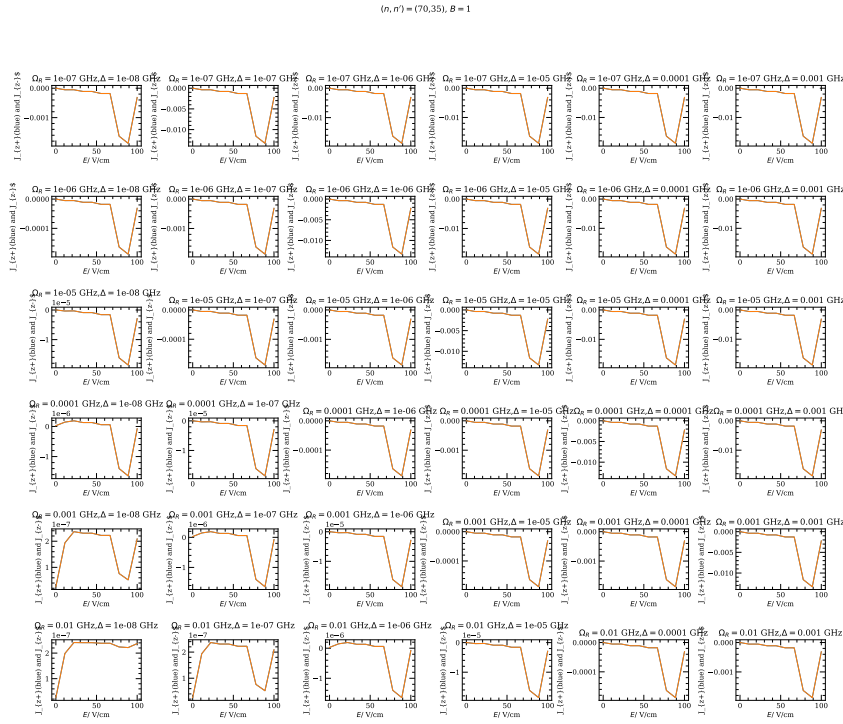


Figure 31:  $J_{+-}/J_{zz}$  as a function of  $\Omega_R$  for  $\Delta = 1\text{kHz}$  and different combinations of  $E, B$

4.2.4  $J_{z+}$  and  $J_{z-}$ 

 Figure 32:  $J_{z+}$  and  $J_{z-}$  as a function of  $B$  for  $E = 1V/cm$  and different combinations of  $\Delta, \Omega_R$ 

 Figure 33:  $J_{z+}$  and  $J_{z-}$  as a function of  $E$  for  $B = 1Gauss$  and different combinations of  $\Delta, \Omega_R$

$(n, n') = (70, 35), Q_{\text{Rabi}} = 0.1$

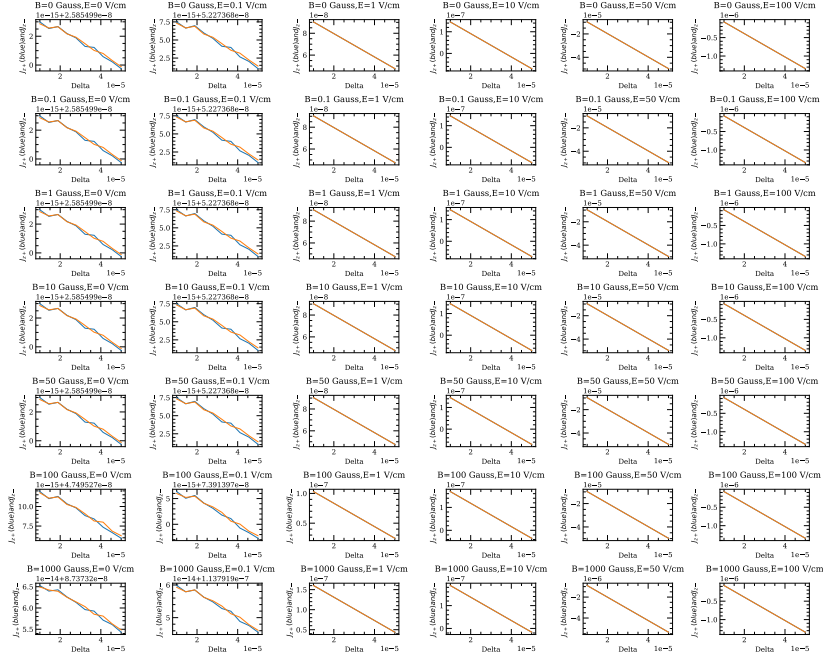


Figure 34:  $J_{z+}$  and  $J_{z-}$  as a function of  $\Delta$  for  $\Omega_R = 0.1 \text{ GHz}$  and different combinations of  $E, B$

$(n, n') = (70, 35), \Delta = 1e-06$

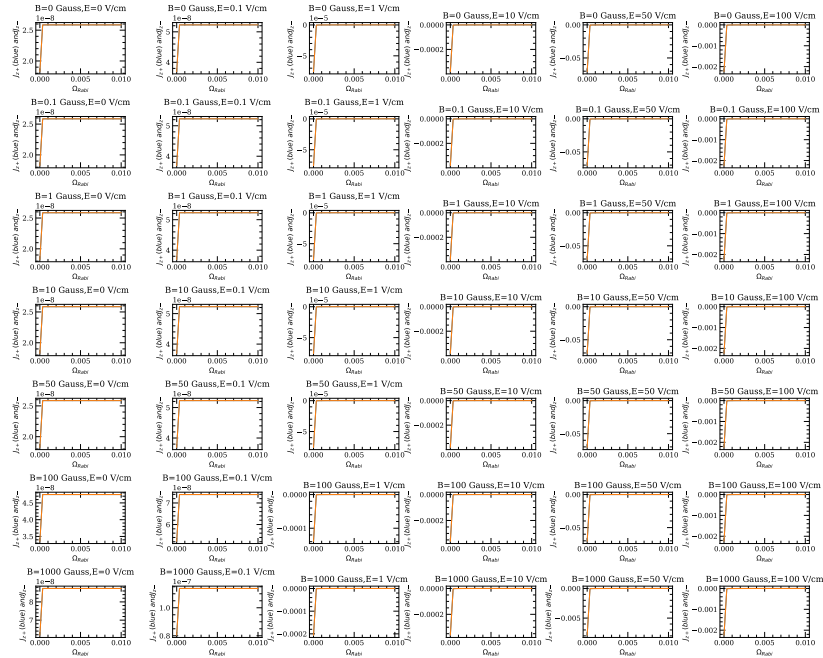
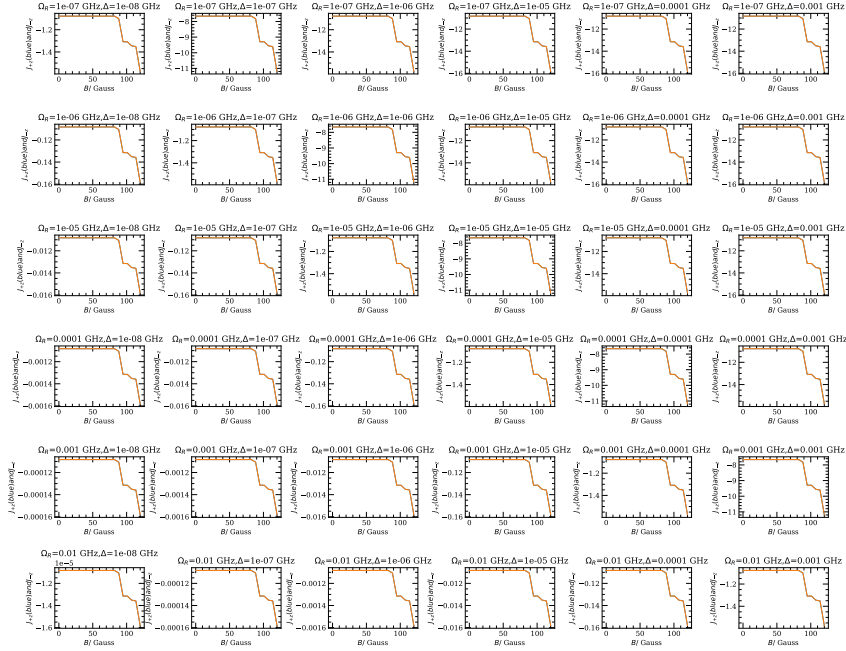
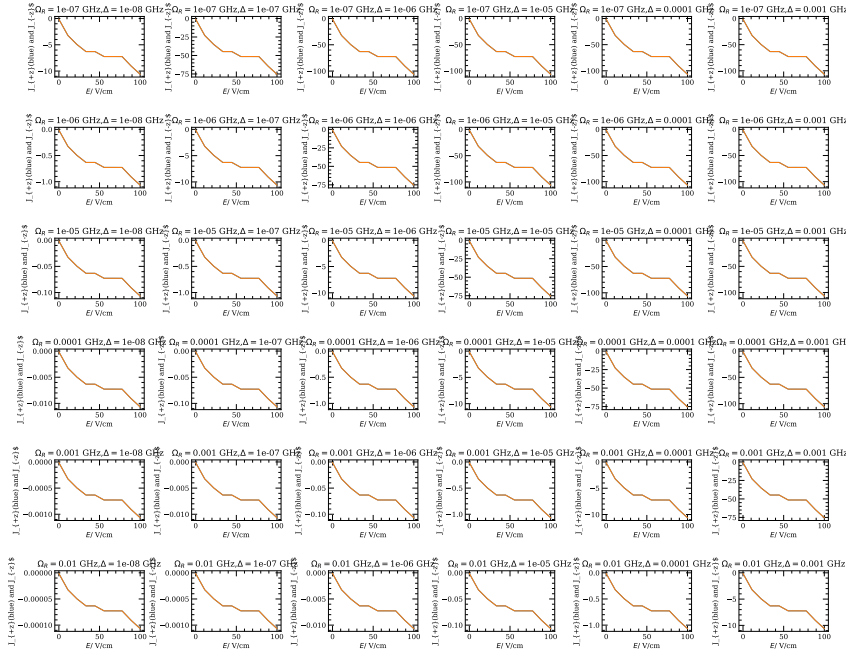


Figure 35:  $J_{z+}$  and  $J_{z-}$  as a function of  $\Omega_R$  for  $\Delta = 1 \text{ kHz}$  and different combinations of  $E, B$

4.2.5  $J_{+z}$  and  $J_{-z}$ 
 $(n, n') = (70, 35), E = 1$ 

 Figure 36:  $J_{+z}$  and  $J_{-z}$  as a function of  $B$  for  $E = 1V/cm$  and different combinations of  $\Delta, \Omega_R$ 
 $(n, n') = (70, 35), B = 1$ 

 Figure 37:  $J_{+z}$  and  $J_{-z}$  as a function of  $E$  for  $B = 1Gauss$  and different combinations of  $\Delta, \Omega_R$

$(n, n') = (70, 35), Q_{\text{Rabi}} = 0.1$

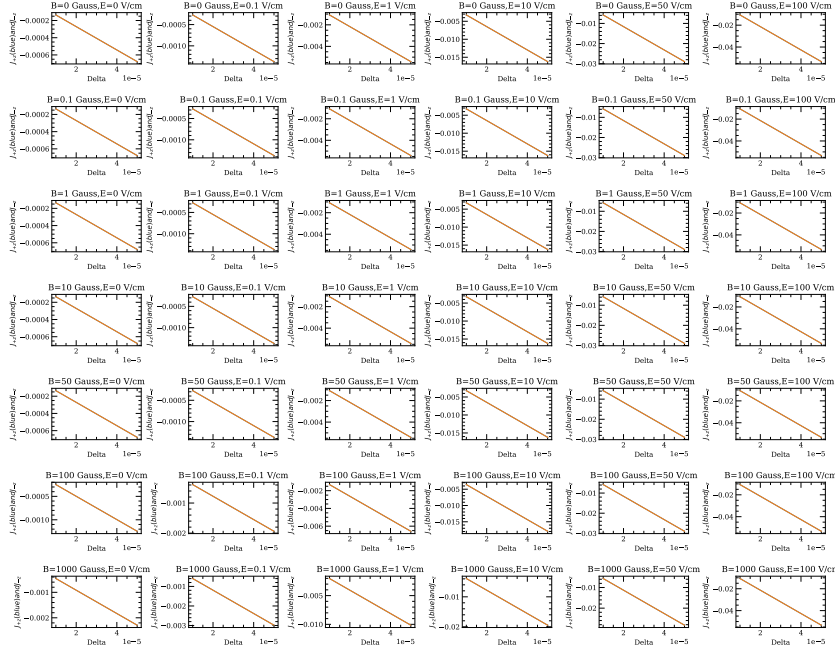


Figure 38:  $J_{+z}$  and  $J_{-z}$  as a function of  $\Delta$  for  $\Omega_R = 0.1GHz$  and different combinations of  $E, B$

$(n, n') = (70, 35), \Delta = 1e-06$

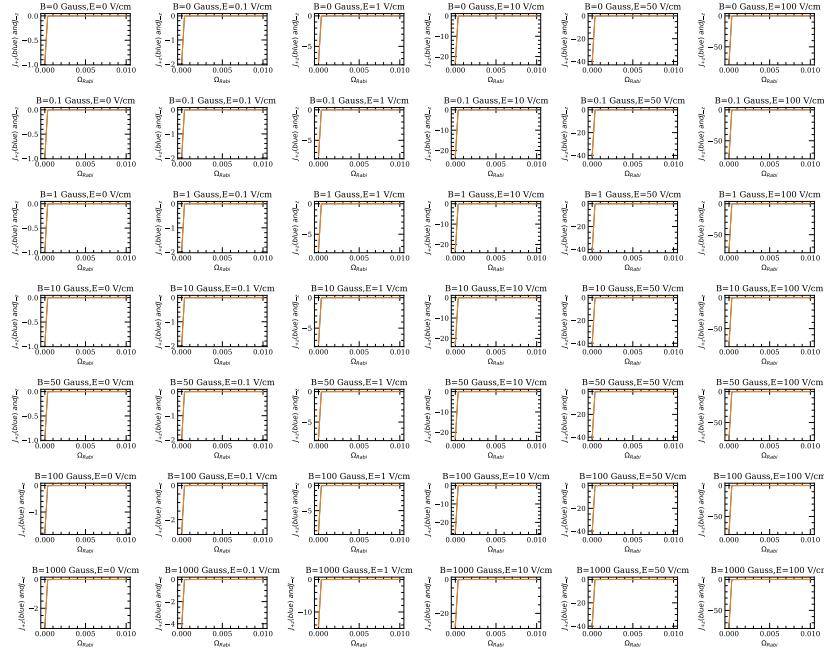
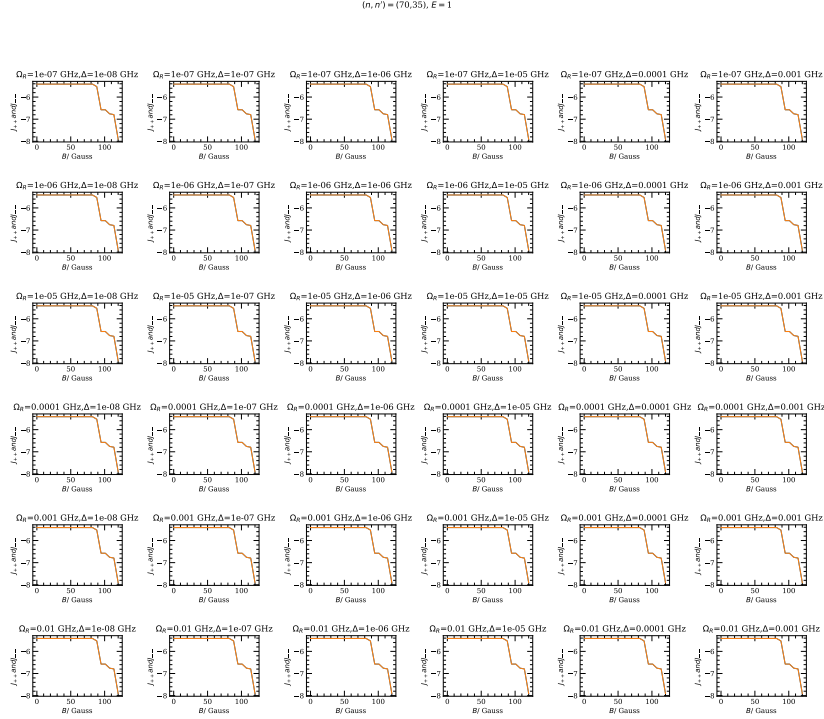
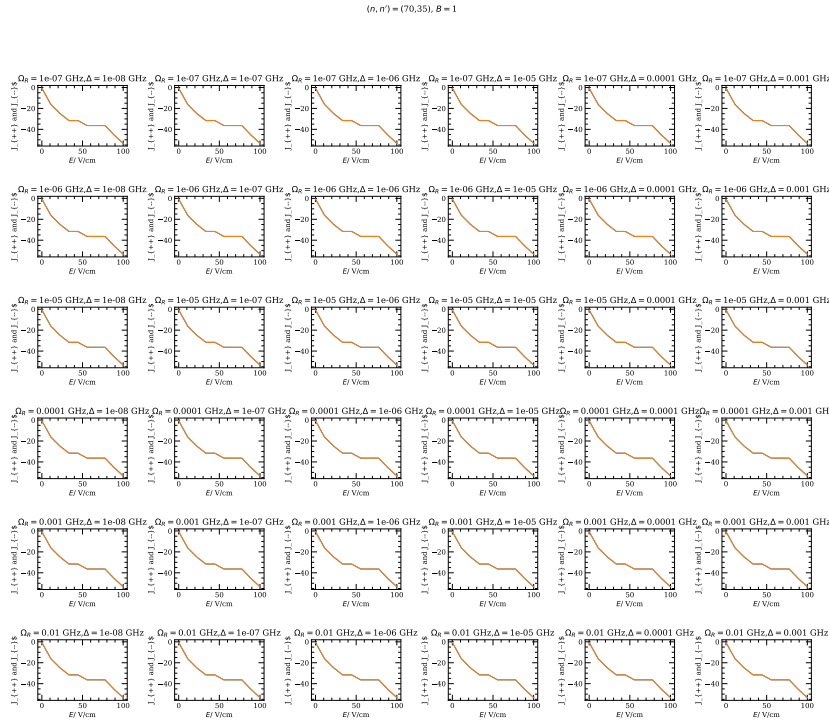


Figure 39:  $J_{+z}$  and  $J_{-z}$  as a function of  $\Omega_R$  for  $\Delta = 1kHz$  and different combinations of  $E, B$

4.2.6  $J_{++}$  and  $J_{--}$ 

 Figure 40:  $J_{++}$  and  $J_{--}$  as a function of  $B$  for  $E = 1V/cm$  and different combinations of  $\Delta, \Omega_R$ 

 Figure 41:  $J_{++}$  and  $J_{--}$  as a function of  $E$  for  $B = 1Gauss$  and different combinations of  $\Delta, \Omega_R$

$(n, n') = (70, 35), Q_{\text{Rabi}} = 0.1$

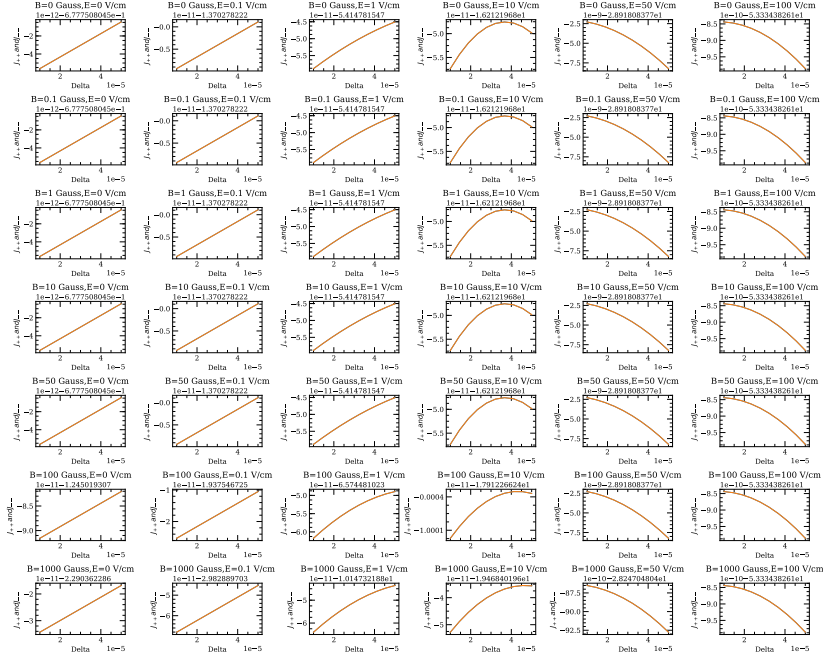


Figure 42:  $J_{++}$  and  $J_{--}$  as a function of  $\Delta$  for  $\Omega_R = 0.1 \text{GHz}$  and different combinations of  $E, B$

$(n, n') = (70, 35), \Delta = 1e-06$

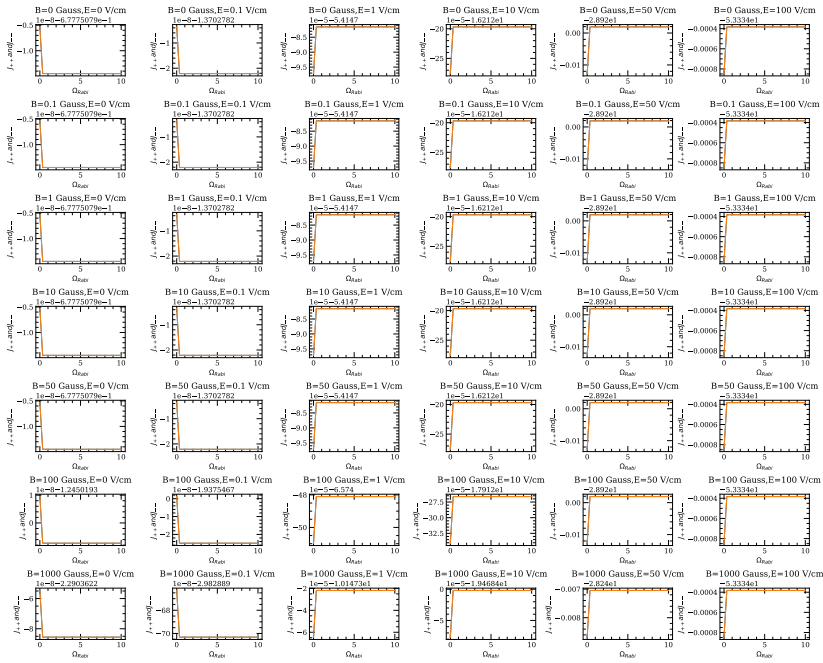


Figure 43:  $J_{++}$  and  $J_{--}$  as a function of  $\Omega_R$  for  $\Delta = 1 \text{kHz}$  and different combinations of  $E, B$

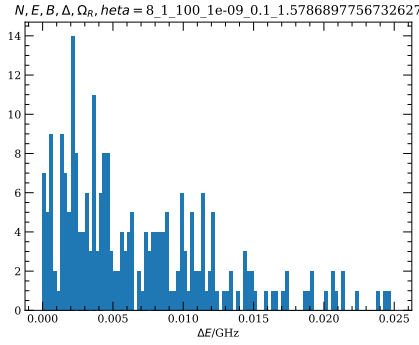


### 4.3 Histograms of eigenvalue differences

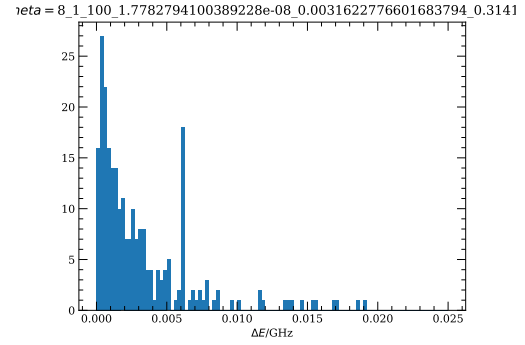
For small numbers of atoms, I determined for various combinations of the external parameters the statistics of the differences of neighbouring eigenvalues. Again, I assumed identical detuning  $\Delta$  and Rabi frequency  $\Omega_R$  for both the central and the bath atom. I did not look at how close to resonance the spin exchange process between the central and a bath atom is.

Very different statistics seem to be possible, a few examples are shown below. However, one should keep in mind that the number of atoms is very small and that relative variations can therefore be large. This should be investigated for larger numbers of atoms, but my own computer does not have the computational capabilities to do so.

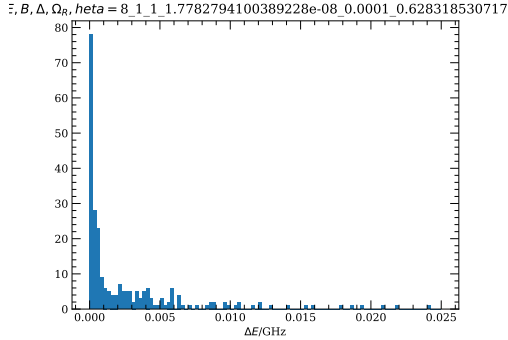
Titles are:  $N, E, B, \Delta, \Omega_R, \theta$ , where  $\theta$  is the angle by which the ring around the central atom is tilted.



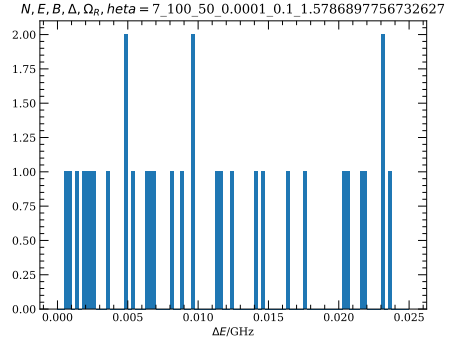
(a)  $N = 8, E = 1V/cm, B = 100Gauss, \Delta = 1Hz, \Omega_R = 0.1GHz, \theta = \frac{1}{1.99}\pi$



(b)  $N = 8, E = 1V/cm, B = 100Gauss, \Delta = 18Hz, \Omega_R = 3.2MHz, \theta = \frac{1}{10}\pi$



(c)  $N = 8, E = 1V/cm, B = 1Gauss, \Delta = 18Hz, \Omega_R = 0.1MHz, \theta = \frac{1}{5}\pi$



(d)  $N = 7, E = 100V/cm, B = 50Gauss, \Delta = 0.1MHz, \Omega_R = 0.1GHz, \theta = \frac{1}{1.99}\pi$

At least under some conditions, enlarging the tilt angle  $\theta$  seems to have the following influence:

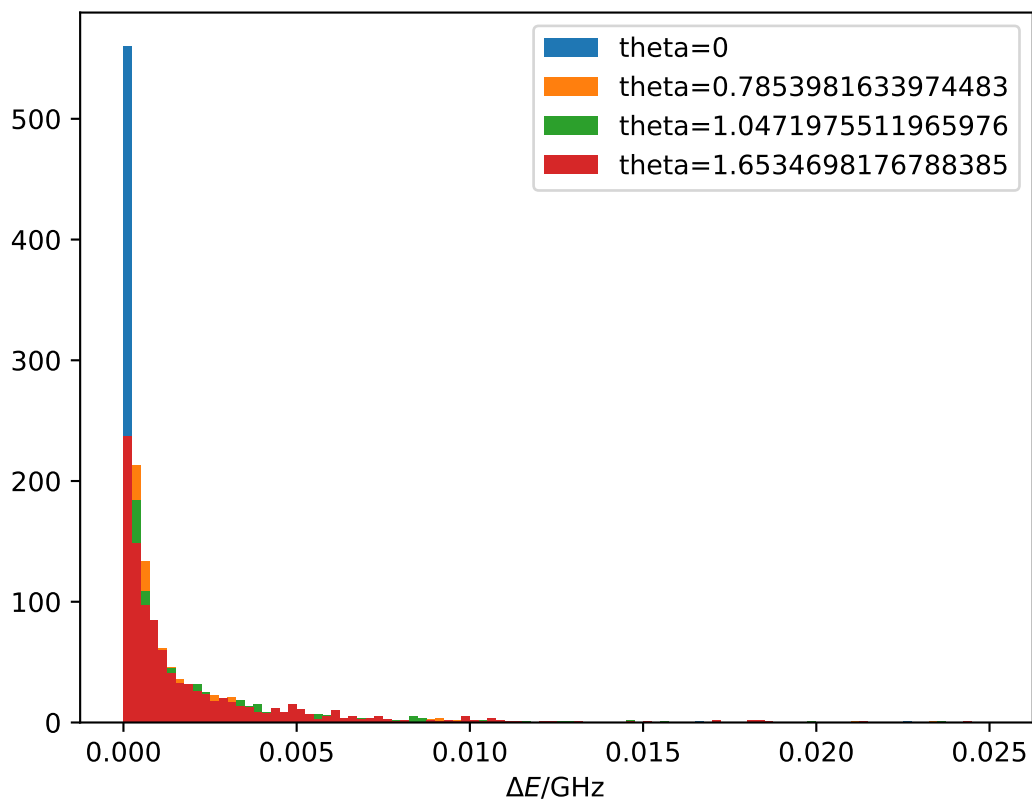


Figure 45: Statistics for different tilt angles. The chosen parameters are  $N = 10, E = 1V/cm, B = 1Gauss, \Delta = 0.1kHz, \Omega_R = 1MHz$

## References

- [Gal94] Gallagher, T. “Rydberg Atoms”. In: *Springer Handbook of Atomic, Molecular, and Optical Physics*. Springer, 1994, pp. 231–240.
- [KP11] Kotochigova, S. and Petrov, A. “Anisotropy in the Interaction of Ultracold Dysprosium”. In: *Phys. Chem. Chem. Phys.* **13** (42 2011), pp. 19165–19170.
- [Mey21] Meystre, P. *Quantum Optics. Taming the Quantum*. Cham: Springer, 2021.
- [Ngu+18] Nguyen, T., Raimond, J., Sayrin, C., Cortinas, R., Cantat-Moltrecht, T., Assemat, F., Dotsenko, I., Gleyzes, S., Haroche, S., Roux, G., et al. “Towards Quantum Simulation with Circular Rydberg Atoms”. In: *Physical Review X* **8** (2018).